KTH ROYAL INSTITUTE
OF TECHNOLOGY

Degree Project in Hydraulic Engineering

Second cycle 30 credits

Groundwater modeling of Krycklan catchment and evaluation of the groundwater discharge distribution

SANDRA EDSTRÖM

Stockholm, Sweden 2022

Authors
Sandra Edström

Place for Project
Degree Project in Hydraulic Engineering, AF283X
KTH Royal Institute of Technology
School of Architecture and Built Environment
Department of Sustainable Development, Environmental Science and Engineering
SE-100 44 Stockholm, Sweden

Examiner
Joakim Riml
Resources, Energy and Infrastructure
KTH Royal Institute of Technology

Supervisors
Anders Wörman
Resources, Energy and Infrastructure
KTH Royal Institute of Technology

Brian Babak Mojarrad
WSP, Hydrogeologist

Abstract

This thesis aimed to evaluate the groundwater discharge distribution in the Krycklan catchment by developing a groundwater flow model using COMSOL Multiphysics and assuming a topography-controlled groundwater surface. Previous research has shown that the groundwater surface can be modeled as a subdued replica of the topography in humid climate regions where the permeability of the subsurface is low and where the groundwater surface is shallow. In earlier studies by Mojarrad (2021), it has been shown that the modeled infiltration becomes higher than the observed infiltration when a topography-controlled groundwater surface boundary is used and that a solution to this is to decrease the resolution in recharge areas. This method was therefore used in the thesis; however, the modeled infiltration was unsuccessfully lowered. This is thought to be due to differences between the model and the previous study and which are discussed further in this thesis. The discharge and recharge areas were identified using the direction of the vertical component of Darcy velocity, and the discharge flow distribution was evaluated in ArcMAP. The discharge flow distribution in the landscape was compared to real geographical data of surface water to identify a discharge threshold value for when the water balance is upheld by surface water flow or by evapotranspiration. The evapotranspiration discharge flow distribution was also evaluated, where the highest flow values were found in riparian zones of the landscape.

Key words

groundwater modelling; groundwater flow; Krycklan catchment; topography-controlled groundwater surface; evapotranspiration; groundwater discharge; groundwater recharge.

Sammanfattning

Syftet med denna avhandling var att utvärdera föredelningen av grundvattnets utflöde i Krycklans avrinningsområde genom att utveckla en grundvattenflödesmodell i COMSOL Multiphysics med antagandet av en topografikontrollerad grundvattenyta. Tidigare forskning har visat att grundvattenytan kan modelleras som en dämpad kopia av topografin i fuktiga klimatområden där permeabiliteten i underytan är låg och där grundvattenytan är grund. En implikation av att använda en topografikontrollerad grundvattenyta har visat sig vara att den modellerade infiltrationen blir högre jämfört med den observerade infiltrationen. Tidigare studier av Krycklans avrinningsområde har visat att genom att minska upplösningen i infiltrationsområden kan den modellerade infiltrationen framgångsrikt sänkas, därför användes denna mesh-utjämningsmetod i avhandlingen. För validering av modellen jämfördes den modellerade infiltrationen med den observerade infiltrationen i Krycklans avrinningsområde. Valideringen visade att mesh-utjämningen misslyckades med att minska infiltrationen, vilket tros bero på skillnader mellan modellen och den tidigare studien och som diskuteras vidare i denna avhandling. Grundvattnets infiltration- och utflödesområden identifierades med hjälp av riktningen på den vertikala komponenten av Darcy-hastighet, och utflödesfördelningen utvärderades i ArcMAP. Utflödesfördelningen i landskapet jämfördes med verkliga geografiska data för ytvatten för att identifiera ett tröskelvärde för utflödet när vattenbalansen upprätthålls av ytvattenflöde eller av evapotranspiration. Fördelningen av utflöden genom evapotranspirations utvärderades också, där de högsta flödesvärdena återfanns i områden nära ytvattenkroppar i landskapet.

Nyckelord

grundvattenmodellering; grundvattenflöde; Krycklan avrinningsområde; topografi-kontrollerad grundvattenyta; evapotranspiration; grundvattenutflöde; grundvatteninfiltration.

Acknowledgements

I am very grateful that I could finish my master's degree with a thesis in hydrogeology, and with guidance from two incredibly competent supervisors. Thanks to my supervisor Anders Wörman, for your guidance, knowledge in hydrology and hydrogeology, support and enthusiasm. Thanks to my supervisor Brian Mojarrad, for your guidance, knowledge in groundwater flow modeling and hydrogeology, your enthusiasm, encouragement, and support. And also, thanks to my examinator, Joakim Riml for your knowledge, input and thoughts!

Table of content

_Toc106634902

Lists

List of figures

List of tables

1 Introduction

Evaluation, observation, and modeling of basin-scale groundwater flow and its controlling factors started in the early 1960s. Later on, it developed into more extensive and deep groundwater basins (Toth, 1999). There are several unique challenges with the modeling and prediction of groundwater systems. A groundwater model can, for example, never be a total replica of a groundwater system because of the system's complexity. The geometry of groundwater systems is usually quite complex with recharge-dependent groundwater divides, which do not always correspond to surface water divides and with the presence of superimposed multiple groundwater systems (Condon & Maxwell, 2015). Several assumptions and simplifications are therefore often required. There are some features of catchments that are especially important to consider and have good representations of if we want to improve the model's predictive capability. These features are the hydrological fluxes, such as recharge, evapotranspiration, interactions with surface water bodies, and the characteristics of aquifers, such as the storativity and hydraulic conductivity. Modeling of areas with shallow groundwater especially requires a robust conceptual representation of the recharge and evapotranspiration since these processes are more pronounced in such areas (Doble & Crosbie, 2016).

Today, there is still limited knowledge of the hydrogeological interactions and states which occur in nature. A common assumption in groundwater modeling is to conceptualize the groundwater table as a subdued replica of the topography (Marklund & Wörman, 2011). Hajitema and Mitchell-Bruker (2005) introduced the concept of classifying the water table as either topography- or recharged controlled, and they found that the groundwater configuration in humid regions, which have high recharge areas, low conductivity, and shallow groundwater tables, are more likely to be controlled by topographic gradients compared to hydraulic gradients. Such an assumption simplifies the reality, as the geology and climate also are factors that affect the groundwater configuration. However, due to sparse groundwater observations, the assumption of a topography-controlled groundwater table enables more or less accurate groundwater modeling for catchments (Condon & Maxwell, 2015). It has been shown that compared to the observed infiltration, the modeled infiltration becomes higher when a topography-controlled groundwater table is used for the top boundary condition. A solution to this is to decrease the resolution of the topography in recharge areas, a form of mesh smoothing, until the modeled infiltration corresponds to the observed infiltration (Marklund & Wörman, 2011).

Evapotranspiration is, as mentioned, also essential to have a good representation of in groundwater modeling. The evapotranspiration rate in riparian zones is affected by many factors, such as the specific characteristics of plants and the available water for root uptake (Nachabe et al., 2005). The evapotranspiration is supported by the continuous supply of water from both precipitation and subsurface flow which is driven by the groundwater dynamics; it has been shown that the rate of evapotranspiration is higher in areas with more shallow groundwater tables (Jayakody et al., 2014; Nachabe et al., 2005). The groundwater dynamics in the riparian zone versus the upslope areas of a catchment differ from each other, emphasizing the need to distinguish between these zones in groundwater modeling, according to Seibert et al. (2003).

1.1 Aim and objectives

The aim for this master thesis is to evaluate the discharge flow distribution in Krycklan Catchment by performing groundwater modelling using COMSOL Multiphysics. Literature research is performed on the hydrological cycle, groundwater flow, previous studies on the research area and on Krycklan catchment.

The objectives are listed below.

- Build a groundwater model of Krycklan Catchment using COMSOL Multiphysics assuming a topography-controlled groundwater surface.
- Define the recharge and discharge areas of Krycklan Catchment.
- Perform a mesh smoothing of the topography resolution in recharge areas.
- Describe the groundwater discharge distribution of the catchment in evapotranspiration- and surface water discharge areas.

2 Theoretical background

The theoretical background aims to cover factors which affect the groundwater flow pattern in catchments, particularly in humid climate regions, and knowledge which are to be a foundation for further understanding of the assumptions and limitations in groundwater modelling.

2.1 Hydrological cycle

The hydrological cycle consists of several different hydrological processes: evapotranspiration, precipitation, and infiltration. All these processes occur simultaneously; however, it can be described as a cycle for simplification. First, water evapotranspiration occurs from land surfaces and oceans into the atmosphere; this water vapor goes through condensation and precipitation onto land or surface water bodies. The precipitated water can then infiltrate through the ground surface, be intercepted by vegetation, or come to be part of overland flow. The infiltrated water becomes soil moisture or subsurface flow. The water which percolates through the subsurface can recharge the groundwater, which, together with overland flow and interflow, discharges into surface water bodies. Evaporation returns the water into the atmosphere. The hydrological cycle occurs both on a local, regional, and continental scale, where the cycles on these scales are interrelated (Chow et al., 1988, pp.2-6).

2.1.1 Precipitation

Rainfall, snowfall, and hail are all different precipitation types that contribute to soil moisture storage, surface water storage, and water that becomes part of overland flow. The normal value of precipitation is calculated by taking the average of the observed value over several years (Chow et al., 1988, pp.71 & 128). The mean annual precipitation for the normal period 1990-2020 in Sweden varies between 400-1200 mm depending on the geographical location, where the coast and the mountainous areas in the east generally have a higher value compared to the rest of Sweden (SMHI, n.d).

2.1.2 Infiltration

Infiltration is the hydrological process of when water from precipitation infiltrates the ground surface. The infiltration rate is controlled by many factors, such as vegetation cover, current soil moisture, land slope, and soil properties like hydraulic conductivity and porosity. The vegetation and the soil moisture vary depending on season and climate, which introduces a temporal variation to both the infiltration rate and, therefore, groundwater recharge. The soil moisture can be stored as both retention storage and detention storage, where retention storage is stored for longer while detention storage is stored for a shorter time. Generally, retention storage is discharged through evapotranspiration, and detention storage is discharged by subsurface- and overland flow towards surface water bodies. Some precipitation is neither stored as retention nor detention; this is called the excess or effective rainfall, which contributes to the direct runoff. Infiltration can be manually measured, for example, by using

tracer tests, and several mathematical functions can be used for estimation of the infiltration, e.g., Green-Ampt equation, Horton's equation, and Philip's equation. The infiltration can also be estimated using the water balance equation, a simplified method where the infiltration becomes equal to the difference between the precipitation and evapotranspiration (Chow et al., 1988, pp. 108; 127-131; 192).

2.1.3 Evapotranspiration

Evapotranspiration is the collective name of the hydrological processes of evaporation and transpiration; it occurs both from land surfaces and surface water bodies. Evaporation from surface water bodies is controlled by the supply of energy, such as solar radiation, for the vaporization of water and by the transport availability, such as wind velocity and specific humidity gradient, of the vaporized water. Evapotranspiration from land surfaces emerges from the vegetation surface, while transpiration is the process of water diffusing into the atmosphere from the stomata, essentially tiny openings, in the leaves of plants (Chow et al., 1988, pp.80-91). The evapotranspiration by vegetation is an important component of the energy balance and water balance at the surface of the earth. Evapotranspiration by vegetation is a large source of water for the precipitation on a global basis, where approximately 60% of the mean precipitation comes from the evapotranspiration by vegetation. Knowledge of evapotranspiration is therefore important on a basin and region scale (Tateishi & Ahn, 1996).

There are different methods for estimation of evapotranspiration; where White (1932) developed a method that focuses on the direct groundwater absorption by plants; however, this requires accurate data of the specific yield, which both can have a temporal and spatial variation, and this can limit the usability and applicability of the method. A method suitable for shallow groundwater areas and a simpler method, as it does not require data of the specific yield, is the implementation of field measurements by monitoring soil moisture with, for example, lysimeters (Nachabe et al., 2005).

2.2 Subsurface flow

Subsurface flow includes the processes of infiltration, interflow (unsaturated flow), and groundwater flow (saturated flow). Interflow occurs above the groundwater table where some of the voids in a porous medium, i.e., soil and rock strata that permit water flow, are filled with air. Groundwater flow occurs below the groundwater table, where the voids are entirely occupied by water. The groundwater surface is the level at which the pressure in a saturated porous medium corresponds to the atmospheric pressure, and below this water table, the pressure increases with depth. The depth of the groundwater table is not constant; it has a temporal variation depending on recharge- and discharge rates. Subsurface flow, together with overland flow, discharges into surface water bodies such as streams and lakes and contributes to the soil moisture in discharge areas. In humid regions with vegetated surfaces, the primary process for water transportation to discharge areas is subsurface flow, this is since the observed precipitation rarely exceeds the soil's infiltration capacity (Chow et al., 1988, pp.129).

2.2.1 Groundwater flow

Groundwater flow naturally has low velocities and low Reynold's number, giving the flow a laminar flow regime (Mojarrad et al., 2021). Its flow pattern, i.e., its spatial distribution, is controlled by both topographic, climatologic, and geologic conditions. The topographic and geologic factors can be assumed as constant in a catchment. In contrast, climatological factors such as precipitation, air temperature, and actual evapotranspiration have a temporal variation. The water table in regions with excess precipitation, e.g., humid regions, can be considered a close replica of the topography (Toth, 1970).

There are three features that characterize each flow system in a catchment and of which the flow pattern can generally be described. These are the recharge limb where infiltrated water descends from the recharge area through the water table in a downward direction; the transfer limb where water is flowing parallel to the water table in a downstream direction; the discharge limb where the water flows upward through the water table towards the discharge area (Toth, 1970). Toth (1963) found that the groundwater flow system in a catchment can be divided into local, intermediate, and regional systems, see Figure 1. The local system has a topographic high as its recharge area and a topographic low as its discharge area, and these are located close to one another. Intermediate systems have several topographic highs and lows between their recharge and discharge areas. A regional groundwater flow system has its recharge area in the proximity of the catchment's main topographical water divide and its discharge area at a surface water body in the downstream regions of the catchment (Toth, 1963).

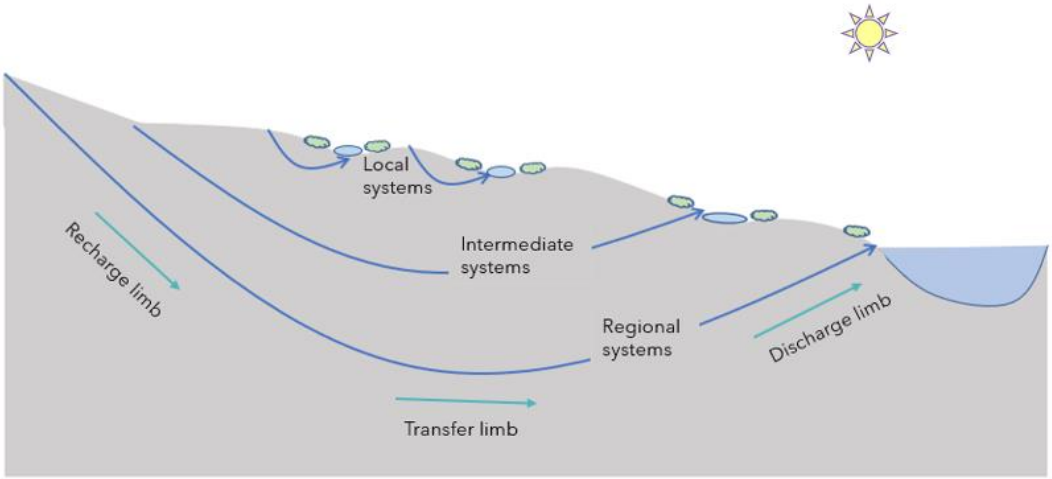

Figure 1 Illustration of the different groundwater systems and the characteristic features (figure modified after Toth (1970)).

2.2.2 Darcy's Law

Darcy's law was developed by Henry Darcy, with the use of experimentation, as an expression of conservation of momentum and was later derived from the Navier-Stokes equations; partial differential equations developed to describe the flow of viscous fluid (Atangana, 2018). Darcy's law is commonly applied in groundwater flow modeling as the governing equation for the flow; the equation is valid for groundwater flow in saturated porous media and for laminar groundwater regimes

$$v = -K\frac{\partial H}{\partial L} \tag{2.1}$$

where v (m/s) is Darcy's velocity, K (m/s) is the hydraulic conductivity, H (m) is the hydraulic head which for groundwater flow is equal to the elevation of the water surface, and L (m) is the distance. The hydraulic conductivity varies in the subsurface, further explained under *2.2.3 Hydraulic conductivities*, and Darcy's law for a heterogenous domain can further be expressed as

$$v = \left(-K_x\frac{\partial H}{\partial x}\right) + \left(-K_y\frac{\partial H}{\partial y}\right) + \left(-K_z\frac{\partial H}{\partial z}\right) \tag{2.2}$$

and assuming steady states conditions and incompressible flow, the continuity equation states that

$$\frac{\partial v_x}{\partial x} + \frac{\partial v_y}{\partial y} + \frac{\partial v_z}{\partial z} = 0 \tag{2.3}$$

which together with Darcy's law in Equation 2.2 gives that

$$0 = \frac{\partial}{\partial x}\left(-K_x \frac{\partial H}{\partial x}\right) + \frac{\partial}{\partial y}\left(-K_y \frac{\partial H}{\partial y}\right) + \frac{\partial}{\partial z}\left(-K_z \frac{\partial H}{\partial z}\right) \quad 2.4$$

which is the governing equation for groundwater flow in a heterogenous saturated porous media assuming steady state conditions and incompressible flow.

2.2.3 Hydraulic conductivity

Geological features in the subsurface are often heterogeneous with local hydraulic conductivity variations. Furthermore, it has been shown that there is a decrease in the hydraulic conductivity with increasing depth in most geological formations and that this decrease has a non-linear nature (Marklund & Wörman, 2011). Saar and Manga (2004) developed an exponential permeability curve that describes the non-linear decrease of the conductivity in geological formations. They proposed an exponential decrease of the permeability in the top 800 m and a power-law function in the subsurface below 800 m, see Equation 2.5 and 2.6 respectively.

$$k(z) = k_s e^{\frac{z}{\delta}} \quad 2.5$$

where k (m/s) is the permeability at depth z (m), k_s (m^2) is the permeability at the ground surface and δ (m) is a decay coefficient. Saar and Manga (2004) suggested appropriate values for k_s and δ to be 5×10^{-13} and 250 respectively.

$$k(z) = k_D \left(\frac{-z}{D}\right)^{-\mu} \quad 2.6$$

where k_D (m/s) is the permeability at some depth z (m), and D (m) and μ (–) are decay coefficients. Ingebritsen and Manning (1999) had earlier presented a power-law function identical to the one proposed by Saar and Manga (2004), and they proposed values for k_D, D, and μ to be 10^{-14}, 1, 000, and 3.2 respectively. The hydraulic conductivity for Quaternary deposits is often assumed to have a spatial variation both since it has heterogeneous properties due to different soil layers and since there is an exponential decay with depth. Bedrock, on the other hand, is often assumed as homogenous in groundwater modeling and therefore only has a spatial variation with depth due to the exponential decay.

2.3 Catchment

A catchment is an area bounded by water divides, such as topographic highs working as its upstream boundaries and a surface water body as its lower boundary into which the water from the area is discharged (Toth, 1963). Groundwater divides are often assumed to correlate with surface water divides since location data is often unavailable for groundwater divides (Erdbrügger et al., 2021a). Features that describe the groundwater motion in a catchment are the penetration depth of present flow systems, the velocity and direction of flow, and the extent and location of both recharge and discharge areas (Toth, 1963). The flow in recharge areas is downward and divergent, while it is converging and ascending in discharge areas which usually have excessive moisture content. In contrast, recharge areas are deficient in moisture content (Toth, 1999). Below, is a theoretical background of the groundwater recharge and discharge areas of a catchment. There is a larger focus in the groundwater discharge areas, since the main purpose of the thesis is to evaluate the groundwater discharge distribution.

2.3.1 Groundwater recharge area

Areas where water from precipitation can infiltrate the surface, percolate through the subsurface and recharge the groundwater are commonly called recharge areas. Coarser soils usually have higher infiltration rates compared to finer soils which have a larger capillary fringe resulting in increased evapotranspiration of the infiltrated water in the unsaturated zone. The groundwater recharge potential in a catchment is increased with higher precipitation as this increases the supply of water to the catchment. Although the storage capacity of the soil can be a limiting factor during intense rainfall, the timescale of a rainfall event, therefore, has an influence as well. When it comes to snowfall, the recharge is delayed until snowmelt (Doble & Crosbie, 2016).

Precipitation data are typically used to estimate the recharge (Marklund, 2009). As described under *2.1.2 Infiltration*, the infiltration can be estimated with the water balance. Non-permeable layers in the subsurface can affect the subsurface pathways; such a layer can be formed due to the presence of soil strata that hold varying physical properties, such as the hydraulic conductivity of a clay layer which is much lower compared to till soils (Chow et al., 1988, p.108). The moisture storage in the unsaturated zone also affects the potential groundwater recharge. A higher moisture content generally increases the proportion of precipitation that recharges the groundwater; however, this impact is not significant when looking at long-term averages. The presence of steeper slopes in catchments often leads to a higher proportion of precipitation which becomes runoff and interflow (Doble & Crosbie, 2016).

2.3.2 Groundwater discharge area

The discharge area is where water is drained from the catchment, usually in the downstream regions. Groundwater discharge occurs in surface waters of the catchment (Mojarrad et al. 2021) and through evapotranspiration from well-vegetated surfaces, so called groundwater evapotranspiration (Meinzer, 1927; Arnold and Allen, 1996; Nichols, 2000; Groeneveld et al., 2007; Tsang et al., 2014). Most studies on groundwater evapotranspiration have been performed in arid to semi-arid regions, where the groundwater evapotranspiration is a more critical component of the water balance compared to humid regions. However, the groundwater evapotranspiration in riparian zones is an important component in both arid and humid regions (Satchithanantham, 2017). Studies of the evapotranspiration from riparian zones are first presented, which is followed up by presentation of studies on groundwater evapotranspiration and thereafter groundwater discharge in surface water.

Riparian zone

A dense vegetation cover generally entails an increased interception and transpiration of the catchment area, therefore increasing the total evapotranspiration of the catchment. In riparian zones, e.g., an area near a stream with a dense vegetation cover, there are three processes that mainly affect the water cycle: uptake of water by vegetation; water storage in vegetation; and evapotranspiration, see Figure 2. The available water sources for plant uptake are groundwater, soil moisture, precipitation, floods, and atmospheric humidity, where the uptake of water is through root absorption and plant interception. However, the dominant source is difficult to identify, and whether the uptake pattern from these sources varies with time or not. The evapotranspiration is not correlated directly to the root absorption as vegetation stores large amounts of water available for evapotranspiration (Tabacchi et al., 2000).

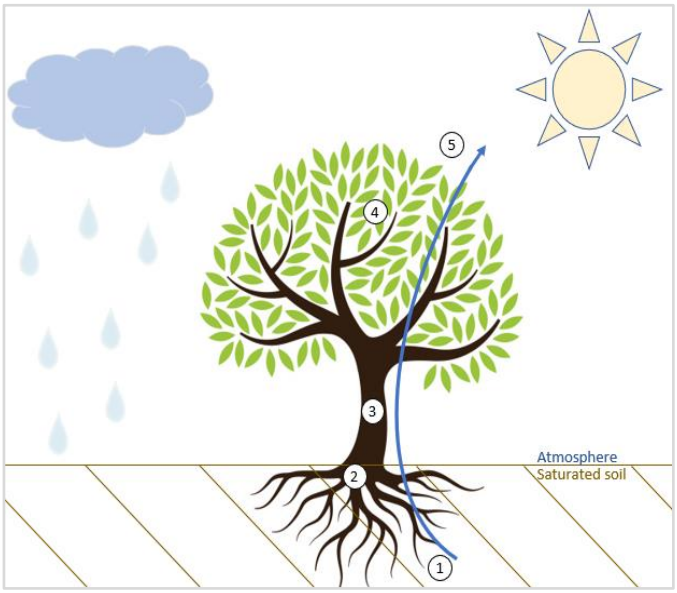

Figure 2 Water cycle of riparian vegetation: 1. Water uptake through roots; 2. Root water storage; 3. Stem water storage; 4. Leaf water storage; 5. Transpiration (figure modified after Tabacchi et al. 2000).

The water consumed by root absorption is replenished by a continuous supply of water from subsurface flow. It has been observed that the depth to the groundwater table decreases during the day due to high evapotranspiration rates in dense vegetative areas, forming a hydraulic gradient that generates a subsurface flow that recovers the groundwater during the night, and which supports the evapotranspiration. Therefore, subsurface flow is an essential contributing factor to the potential evapotranspiration rate of riparian zones, especially in areas with shallow water tables (Jayakody et al., 2014; Nachabe et al., 2005).

Riparian zones can be identified with the help of field excursions and maps showing topography, land use, and aerial photography to identify vegetation covers. The evapotranspiration has a temporal variation (both diurnally and seasonally) and a variation depending on the plant species, where the tree layer, compared to herb- and shrub layers, accounts for the largest evapotranspiration in riparian vegetation (Tabacchi et al., 2000). The evapotranspiration rate in floodplain forests is generally close to the potential rate (Tabacchi et al., 2000) and the evapotranspiration in forested catchments is higher than in grassed catchments (Zhang et al., 2001). Seibert et al. (2003) emphasize the difference between the groundwater dynamics of the riparian and upslope areas of a catchment in humid boreal regions. The groundwater table's temporal variation has shown to be less in riparian zones compared to the variation seen in upslope areas since there is a continuous water supply from the upslope areas. Therefore, Seibert et al. (2003) argue for the importance of this knowledge in groundwater modeling and distinguishing between riparian and upslope zones.

Groundwater evapotranspiration

For arid and semi-arid groundwater basins, the dominating component of the groundwater discharge is often the groundwater evapotranspiration. The water balance can be upheld by groundwater evapotranspiration for closed basins in such regions, where the groundwater evapotranspiration is almost equal to the recharge from precipitation. The accuracy of the spatial quantification of groundwater evapotranspiration are therefore especially important for such regions (Groeneveld et al., 2007; Kurc & Small, 2004), but measurements of the groundwater evapotranspiration are difficult, and such data are not easily accessible which can make it harder to incorporate this component into models (Tsang et al., 2013).

Plant species which have their roots under the groundwater surface, or in the capillary fringe just above it, are called phreatophytes which utilizes the shallow groundwater. There are also plant species that use groundwater only under certain circumstances and plants which uses hydraulic redistribution to induce upward water movement (Meinzer, 1927 & Tsang et al., 2013). The distinction of which species that utilizes groundwater are more pronounced in arid regions, compared to humid regions. But phreatophytes have a critical impact on the water balance of the riparian zones both in arid and humid regions (Satchithanantham, 2017). The type of plant species can both indicate occurrence of groundwater and the depth to the groundwater surface, as some species can utilize deeper groundwater while some uses shallow groundwater. The groundwater evapotranspiration varies depending on the plant species, the weather conditions, the alkali content and texture of the soil, and the depth to the water table (Meinzer, 1927).

The distinction between whether it is groundwater or soil moisture in the unsaturated zone that is utilized by vegetation is not definite, partly due to temporary and perched groundwater surfaces (Meinzer, 1927). However, the common assumption is that with increasing depth to the groundwater surface, there is a decay of the groundwater evapotranspiration. A linear relation of the decay has traditionally been assumed, however Shah et al. (2007) found that an exponential relationship is more suited for estimation of the depth dependency on groundwater evapotranspiration. The spatial extent of groundwater evapotranspiration covers the riparian zones and areas where plants can utilize groundwater, such as shallow groundwater areas (Tsang et al., 2013).

Studies by Lee (1912) and White (1932) are two of the earliest studies which performed estimation of evapotranspiration from the bare soil, saltgrass and native shrubs. Studies which analyze evapotranspiration rates from different plant species usually includes the evapotranspiration of both soil moisture and precipitation, for the analysis of determining the groundwater evapotranspiration such studies are therefore less useful (Nichols, 2000a). Earlier studies by Nichols (1992b, 1993, 1994 & 2000) estimated the groundwater evapotranspiration by rangeland- and phreatophytes shrubs which utilizes shallow groundwater in arid regions. In earlier studies, Nichols (2000b) found that for arid regions, an important component of the water budget is the groundwater evapotranspiration especially by phreatophytes, and the surrounding bare soil. He also found that groundwater evapotranspiration is correlated to denser vegetation covers, and denser vegetation covers are correlated to shallow groundwater, but that there is a weaker correlation between groundwater evapotranspiration and a shallow groundwater. While for evaporation from soil, a shallow groundwater table gives a higher evaporation (Nichols, 2000b).

Tsang et al. (2014) examined the relationship between the topography and the groundwater evapotranspiration and found that the groundwater evapotranspiration was larger in flatter areas with shallow groundwater for a catchment located in a humid region. They found that the groundwater evapotranspiration stood for approximately 6-18 % of the total evapotranspiration, and that the main proportion of the groundwater evapotranspiration occurs over an area of 10% of the total catchment. They also found that, by incorporating groundwater evapotranspiration in a model, that the stream discharge simulation improved, and that the water balance becomes more closely balanced. Tsang et al. (2014) argue that if the groundwater evapotranspiration is neglected in water balance calculations for catchments, this component will either be underestimated or that estimates of the water storage component will be distorted. Compared to result of Tsang et al. (2014), studies by Arnold and Allen (1996) showed similar result for three different catchments in a humid region, the groundwater evapotranspiration accounted for 3.6 %, 8.4 % and 13 % of the total evapotranspiration.

Surface water

Surface water can be identified with field excursions and aerial photography, but also with maps showing topography and land use. For forested catchments, it is often assumed that subsurface water flow paths are the primary process which water is transported through from land to surface waters (Leach et al., 2017). Particle tracing of deep groundwater flow in Krycklan catchment by Mojarrad et al. (2021) showed that deep groundwater discharge is mainly in streams or lakes, and in the downstream regions of the landscape. Lyon et al. (2012) found a spatial variability of the specific discharge in the Krycklan catchment, where smaller sub-catchments, especially headwaters, had more significant variability than the larger sub-catchments. Therefore, they argue that it would be inaccurate to set one uniform specific discharge for the whole catchment. The groundwater flow direction near streams is usually assumed to be in the hillslope direction; however, Rodhe et al. (2011) found that the direction of the groundwater flow changes with varying groundwater levels, where a perpendicular direction towards the stream was found during rising groundwater levels, and a more downstream direction parallel to the stream during falling groundwater levels.

2.4 Groundwater modelling

In this section the theoretical background for the hydrological boundaries and computational methods which are used in the groundwater modelling of this thesis is presented.

2.4.1 Boundaries in groundwater modelling

Groundwater flow problems are solved by partial differential equations that govern its flow movement. To solve these equations, it is essential to define the boundaries of the model domain and specify the head or head gradient along these boundaries. Three of the most commonly applied boundary types are mathematically classified into Dirichlet, Neumann, and Cauchy boundary conditions (BC) (Jazayeri & Werner, 2019).

Dirichlet BC is also commonly called specified head boundary; this refers to a specified head boundary or constant head boundary and can also be applied as a specified or constant pressure head boundary. In groundwater models, the most common application of this boundary is for surface water bodies and where the hydraulic head is not affected by groundwater fluctuations (Jazayeri & Werner, 2019).

Neuman BC is also commonly called specified flow boundary; this refers to a boundary with a specific discharge or Darcy velocity. The volumetric flux can also be set normal to the boundary, and Neumann BC is usually applied for recharge boundaries and base flow. A particular case of Neuman BC is the no-flow conditions, where q is set equal to zero. This condition is also commonly called the zero-flow boundary and is usually applied to represent geological discontinuities, hydraulic divides, and low-permeability strata (Jazayeri & Werner, 2019).

The Cauchy BS is also commonly called the specified leak boundary; this refers to flux through a head-dependent boundary such as leakage through a resistance layer between a surface water body and an aquifer. The relation between the hydraulic head in the aquifer and the leakage through the resistance layer can mathematically be described by the Cauchy BC (de Lange, 1999).

2.4.2 Topography controlled groundwater table

Flow is driven by gravity, the extent to which gravity affects groundwater flow is influenced by the topography and geology of the area. In humid climates and areas with shallow groundwater and low bedrock permeability, the influence of the topography on the groundwater flow is more pronounced, and the groundwater surface can therefore be assumed as a subdued replication of the topography. A

topography-controlled groundwater table can be implemented using digital elevation models (DEMs) for the top boundary condition in numerical groundwater models. This means that the top boundary's hydraulic head in groundwater models is assumed to be equal to the topography elevation data, making the whole domain fully saturated. Furthermore, high-resolution DEM and accurate elevation data are usually easily accessible compared to precipitation data (Marklund, 2009). Hajitema and Mitchell-Bruker (2005) introduced the concept of classifying the water table as either topography- or recharged controlled and derived a dimensionless criterion the water table ratio WTR expressed as

$$WTR = \frac{\Delta h}{d} = \frac{RL^2}{mKHd} = \left\{ \begin{matrix} >1 \; for \; topography \; controlled \\ <1 \; for \; recharge \; controlled \end{matrix} \right\} \quad 2.7$$

where Δh (m) is the groundwater mounding, d (m) is the maximum terrain rise from the average groundwater surface, R (m/d) is the areal recharge rate, L (m) is the distance between surface water bodies, K (m/d) is the hydraulic conductivity, H (m) is the average vertical aquifer thickness, d (m) is the maximum terrain rise and m (unitless) is either 8 or 16, for a one-dimensional or radially symmetric flow problem, respectively. This is illustrated in Figure 3 below

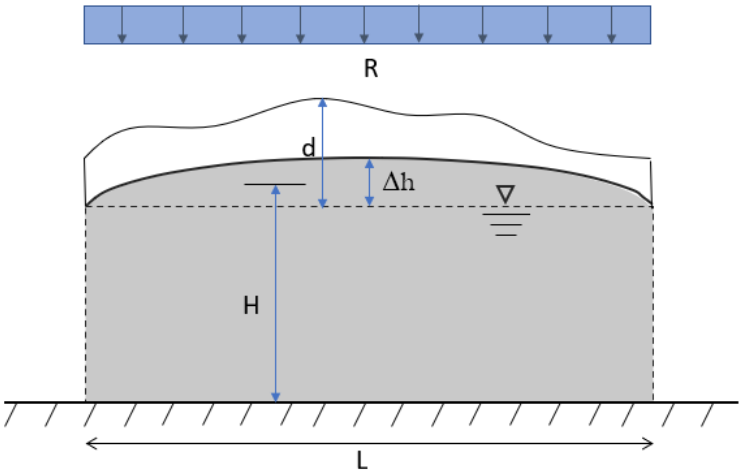

Figure 3 Illustration of groundwater mounding in recharge area (modified after Hajitema and Mitchell-Bruker (2005)).

The knowledge of how and to which extent the topography controls the groundwater flow is limited, and this can create both conceptual- and systematic errors (Marklund, 2009; Marklund & Wörman, 2011). Therefore, the assumption of a topography-controlled groundwater surface entails a complication with the accuracy of the groundwater model. It has been shown that the modeled infiltration becomes much higher compared to the observed infiltration. This is related to the fact that the groundwater surface's relief varies less than the actual topography and that the microtopography found in the topography only affects the groundwater flow directions to a smaller extent (Marklund & Wörman, 2011). Also, systematic bias error can occur in areas where the groundwater table is not topography controlled. The dominant hydrologic process in the area might have a finer or coarser scale than the modeled one (Condon & Maxwell, 2015).

Mesh smoothing

A method to improve the accuracy of the infiltration when using high-resolution DEMs as the top boundary condition is to decrease the variance of the topography. This, in turn, should change the variance of the groundwater table in the model. A higher resolution results in more significant groundwater recharge fluxes due to the higher velocities that occur because of the small-scale undulations and microtopography that can be accounted for only with a higher resolution. The resolution can be decreased in recharge areas until the modeled infiltration corresponds to the observed

infiltration. This aims to achieve a more accurate infiltration for groundwater modeling where a topography-controlled groundwater surface is assumed (Marklund & Wörman, 2011). This applies a Neumann boundary condition in recharge areas and a Dirichlet boundary condition in discharge areas.

Implementation of lower resolution DEM and pre-processing of DEMs have been found to decrease the accuracy of the spatial extent of stream networks, and this affects the scale of drainage areas in smaller catchments which in turn affects the catchment boundaries (Lidberg et al., 2017; Erdbrügger et al., 2021a). Erdbrügger et al. (2021a) found that the groundwater flow direction in some areas of the catchment was explicitly affected by DEM smoothing and aggregation; these were areas where the local topographic relief differed from the general slope gradient, flat areas, and areas near bridges and incised stream banks in the catchment.

Wörman et al. (2007) found that the subsurface flow is influenced both by small-scale and large-scale topography. The effect of microtopography attenuates with depths, which means that larger-scale topography features primarily control deeper groundwater flow. They also found that small-scale topography generally has steeper slopes than large-scale topography. This microtopography is smoothed out when the resolution is decreased, which would result in a smaller mean slope of the landscape when mesh smoothing is applied. Wörman et al. (2007) also found that for a sinusoidal shaped top surface and isotropic harmonic functions, the maximum velocity is equal to

$$\max\left(W_{i,j}(x,y,z=0)\right) = -2\sqrt{2}\pi KB\frac{(h_m)_{i,j}}{\lambda} \tag{2.8}$$

where W (m/s) is the velocity, K (m/s) is the hydraulic conductivity, h_m is the amplitude, B is equal to $\left[1-\exp\left(-2\sqrt{2}\pi\varepsilon/\lambda\right)\right]/\left[1+\exp\left(-2\sqrt{2}\pi\varepsilon/\lambda\right)\right]$ and λ is the wavelength. As the depth to the impermeable surface exceeds $\lambda/3$, the B factors approaches unity. This shows a relationship between the infiltration at the top surface, the hydraulic conductivity, and the slope $s{\sim}h_m/\lambda$:

$$W{\sim}K\cdot s \tag{2.9}$$

3 Conceptual model

In this study, the software COMSOL Multiphysics was used to create a groundwater model representing the groundwater system of Krycklan Catchment located in the North of Sweden, see Figure 4. The model is built up with high-resolution DEM describing the topography of the surface and bedrock. The heterogeneity of the Quaternary deposits and the bedrock is accounted for by implementing a decay function of the hydraulic conductivities, see 2.2.3 Hydraulic conductivity. The groundwater surface is assumed to be a subdued replica of the topography. The resolution in recharge areas was decreased with the aim of decreasing the modeled infiltration. The recharge and discharge areas are identified by evaluating the direction of the vertical component of Darcy velocity at the top surface. The distribution of the groundwater discharge is evaluated by comparing the distribution to the location of the stream network and tree cover volume in Krycklan catchment.

Figure 4 Map showing the location of Krycklan Catchment in Sweden (Lantmäteriet: Min Karta, 2022).

3.1 Study area - Krycklan catchment

Krycklan catchment is located in the north of Sweden, approximately 50 km northwest of Umeå city, and has an area of about 6970 ha. For decades, the catchment has been a subject of research, with forest research dating back to the beginning of the 20th century. Several measurements have been conducted using Light Detection and Ranging (LiDAR), which has increased the availability of high-resolution DEM of the area, and several installations of groundwater wells in the catchment, which promotes continuous scientific research of the area. The catchment has a cold temperate humid climate with a mean annual temperature of 1.8 C between 1981-2010 (Laudon et al., 2013). According to the water balance by SMHI: waterwebb (2020), the mean annual precipitation is about 734 mm, the mean annual runoff 385 mm, and the mean annual evapotranspiration 349 mm.

Krycklan catchment is classified as a forested catchment since 87% of it is covered by forest, with the rest of its surface covered by 9% mires, 7% thin soils, and 1% rock outcrops. The dominant tree species in the forest areas are Scots pine (Pinus sylvestris) and Norway spruce (Picea abies). Svecofennian gneissic bedrock with metasediments and metagraywacke dominates the bedrock of the catchment, which is mainly covered by Quaternary deposits of till and peat at higher altitudes and by postglacial sedimentary deposits at lower altitudes, see figure 5. The depth of the sediments varies between 5-40 meters, and the altitude varies between 114 to 405 m a.s.l in the catchment, see figure 6. There are many small streams in the area which lead the water from the sub-catchments to the river network, see figure 6. The dominating land use is forestry, and most of the area is covered by second-growth forest, where clear cuts cover 7% of the catchment area, and only 25% of the whole area is protected. Although, except for forestry, there is low human impact in the catchment considering the population of 100 people and only 2% arable land (Laudon et al., 2013). The tree volume is illustrated in Figure 7.

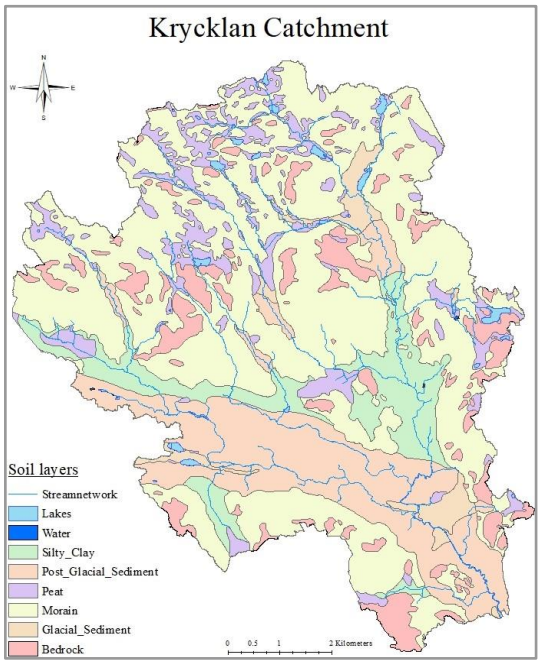

Figure 5 Map over Krycklan Catchment illustrating soil layers, the bedrock outcrop and the stream network.

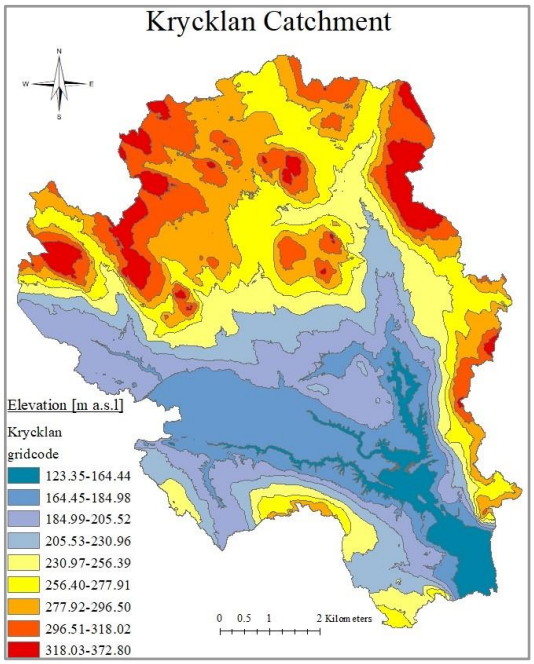

Figure 6 Map over Krycklan Catchment illustrating elevation range in metre above sea level.

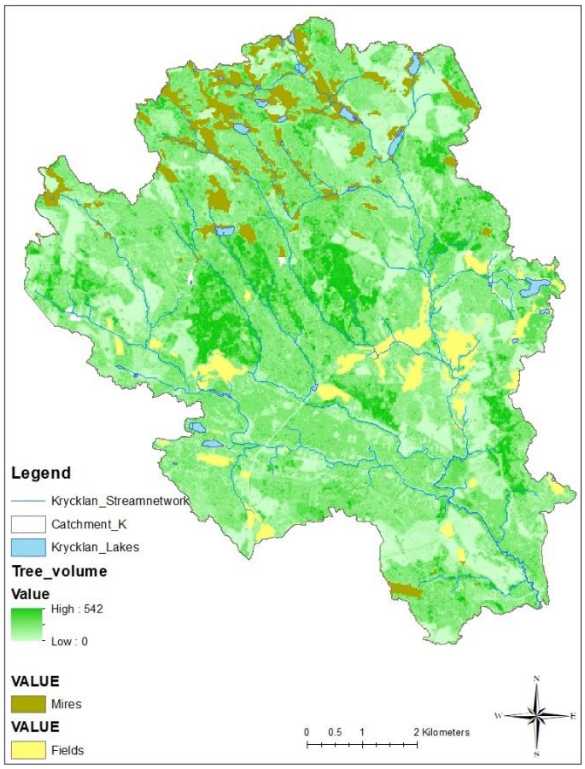

Figure 7 Map showing total tree volume (m3sk/hektar) in Krycklan catchment, were m3sk is Skogskubikmeter i.e., Forestsquaremeter (SLU, 2010).

3.2 Assumptions and limitations

The limitation of this study is the accuracy of the data mentioned under 3.3. Data, the geometry building algorithm of COMSOL, and the computational costs of COMSOL. In COMSOL, the algorithm for building geometry uses a max number of knots and a corresponding required relative tolerance between the actual data and the modeled data. This thus limits the accuracy of the modeled geometry to the DEM. The requirements of RAM memory for computation in COMSOL partly vary depending on the required mesh element size. A finer mesh size results in more accurate modeling and requires more RAM memory. Due to the limitations of the computer, which was used for this thesis, it was not possible to attain a fine enough mesh to accommodate high-resolution DEMs. The assumptions of this study are listed below

- the groundwater surface is shallow
- the flow is fully saturated and incompressible
- the groundwater table is a subdued replicate of the topography
- the soil domain is of porous media which is isotropic and heterogeneous
- and the bedrock domain is isotropic and homogeneous.

3.3 Data

The data used in the thesis and their purpose are listed in table 1 below.

Table 1 The required data for the groundwater model and its purpose.

Data source	**Unit**	**Purpose**
Surface elevation data [1]	[tiff-files]	Model geometry; Top boundary condition
Bedrock elevation data [1]	[tiff-files]	Model geometry
Observed infiltration [2]	[mm/yr]	Infiltration validation
Observed precipitation [2]	[mm/yr]	Calculation of observed infiltration
Observed evapotranspiration [2]	[mm/yr]	Calculation of observed infiltration
Hydraulic conductivity [1]	[m/s]	Domain properties
Land use data [1]	[shp-files]	Groundwater discharge distribution

[1] Mojarrad et al. (2021); [2] SMHI: Waterwebb 2020

3.4 Water balance

The water balance equation is a common and simple method used for estimating a catchment's hydrological responses

$$R = P - ET - \Delta S \tag{3.1}$$

where R (mm/yr) is total runoff, P (mm/yr) is precipitation, ET (mm/yr) is evapotranspiration and ΔS (mm/yr) is change in soil water storage of the catchment. The total runoff includes runoff from the baseflow, interflow and overland flow. The hydrological processes of precipitation, evapotranspiration, and infiltration (contributing to the subsurface flow and water storage) both has temporal and spatial variations in a catchment which affects the water balance. Including this temporal- and spatial variation, the water balance becomes

$$R(\mathbf{X}, t) = P(\mathbf{X}, t) - ET(\mathbf{X}, t) - \frac{\Delta S(\mathbf{X}, t)}{\Delta t} \tag{3.2}$$

where **X** (m) is a vector which defines the location in the landscape, t is the time (s), R (m^3/s) is total runoff, P (m^3/s) is precipitation, ET (m^3/s) is evapotranspiration and ΔS (m^3/s) is change in soil water storage, over a defined volume of land. The change in water storage ΔS becomes negligible as the water balance is averaged over a long period (Zhang et al., 2004), giving that

$$R(\mathbf{X}, t) = P(\mathbf{X}, t) - ET(\mathbf{X}, t) \quad 3.2$$

In this thesis, the water balance is only used for estimation of the infiltration, see 4.2.3 Infiltration.

The conceptual model of this thesis was developed from that the groundwater flow is discharge not only in surface water bodies, but also through groundwater evapotranspiration. This has been showed by earlier studies, Tsang et al. 2014 and Arnold and Allen (1996) in humid regions, and Nichols (2000) in arid to semi-arid regions. The water balance for catchments in arid to semi-arid regions can be upheld by groundwater evapotranspiration, where it has been shown that the groundwater evapotranspiration can be almost equal to the recharge from precipitation (Groeneveld et al., 2007; Kurc & Small, 2004 and Nichols 2000). And literature show that groundwater evapotranspiration is also a critical component of the water balance especially in riparian zones of the landscape in humid regions (Satchithanantham, 2017 and Tsang et al., 2014). This is also supported by that there are different groundwater flow systems as identified by Toth (1963), where local and intermediate systems can discharge groundwater in topographic lows which are not defined as the catchments main discharge area which usually in humid regions is a surface water body of some kind. Since this thesis aims to investigate the discharge flow distribution, the conceptual model has three different areas where the discharge area is divided into two types of areas. One discharge area is surface water bodies where the groundwater is discharge by surface water flow. The other discharge area is the evapotranspiration balanced area where the groundwater is discharge through evapotranspiration, and where the water balance possible can be upheld by evapotranspiration. A schematic illustration of the conceptual model is in Figure 8 below, where the groundwater flow is represented by the component D (m/s).

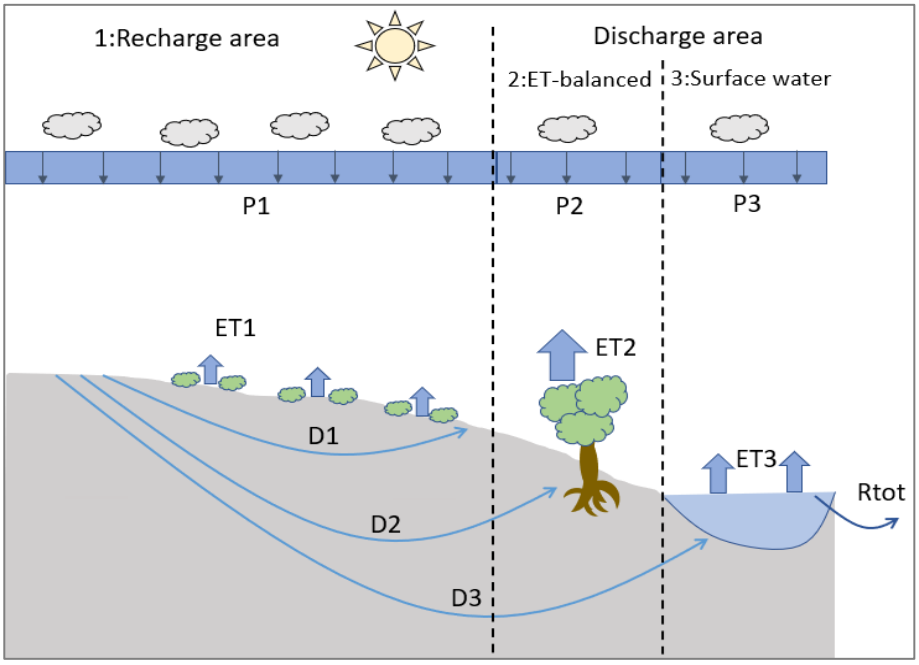

Figure 8 Illustration of the components in the water balance, groundwater flow direction, discharge- and recharge areas.

The actual water balance in a catchment is affected by climatic factors and catchment properties. The climatic factors are precipitation, air temperature, solar radiation, wind speed, and humidity and their temporal variation impact. While vegetation characteristics and physical features are catchment properties. The distribution of precipitation between runoff and evapotranspiration is affected by the soil's permeability and water storage capacity, as well as the topography, where a steeper slope can lead to higher amounts of the precipitation distributed as runoff. The leaf area, plant structure, stomatal functions, radiative properties, and rooting depth are vegetation factors that also affect the water balance. The interactions and feedback of these factors and their spatial variability and combined effect induce complexity in building a groundwater model. The internal storage of immobile water for long periods, such as snow and ice, also introduces complexity (Zhang, 2004).

4 Methodology of groundwater modelling

The groundwater model is created to replicate the groundwater system of Krycklan catchment. The following subsections describe the creation and computation of the model. The work is an iterative process, with computation of the model in COMSOL, defining the recharge and discharge areas, decreasing the resolution of the recharge areas using the software ArcMAP, revision of the bedrock topography in the software Surfer, and so on.

4.1 COMSOL geometry build

The model's geometry was built to avoid intersections between the topography and the bedrock to avoid internal errors in COMSOL. Intersections can occur in areas where the bedrock DEM has the same elevation values as the topography DEM, or where the bedrock rises above the topography. A limitation with COMSOLs geometry building algorithm is that the software cannot handle such intersections very well, as additional domains are created of these intersections when the mesh is built which was not desired in this thesis. The bedrock layer was therefore revised in such intersection areas using the software Surfer, where the areas of intersection were lowered to beneath the topography, and in COMSOL where the whole bedrock layer was lowered. The same method for revision of the bedrock was also performed in the study by Mojarrad et al. (2021) and was therefore deemed acceptable. The data of the surface and revised bedrock DEMs was imported as elevation (DEM) functions, and two domains were created: a top domain for the Quaternary deposits and a bottom domain for the bedrock.

4.1.1 Domain properties

Separate fluid and matrix properties were created for the Quaternary deposits and the bedrock. The density corresponds to water's density, 1000 kg/m^3 for both domains, while the porosity for the Quaternary deposits are 0.2 (Lind & Nyborg, 1986 p.12) and for the bedrock 0.001 (Fitts, 2013). The exponential decay of the hydraulic conductivity for the Quaternary deposits and the bedrock was implemented in the model with the decay function developed by Saar and Manga (2004) and further suggested by Mojarrad et al. (2021)

$$K_i(z) = K_{(Q\ or\ B),top}\, e^{\frac{z - z_{top,i}}{\delta}} \tag{4.1}$$

where $K_i(z)$ is the hydraulic conductivity at depth z (m) for the corresponding soil layer i, $k_{(S\ or\ D),top}$ (m^2) is the permeability at the top surface of either the Quaternary deposits Q or bedrock B, an $z_{top,i}$ is the elevation of the soil layer i at the top surface and δ (m) is a decay coefficient. Saar and Manga (2004) suggested a values for δ as 250 which is used in this study. The hydraulic conductivities were provided

by Mojarrad et al. (2021) where the heterogeneity in the Quaternary deposits was accounted for by referencing the hydraulic conductivity at the top boundary surface to the different soil layers. See figure below for illustration of the hydraulic conductivity variation in depth.

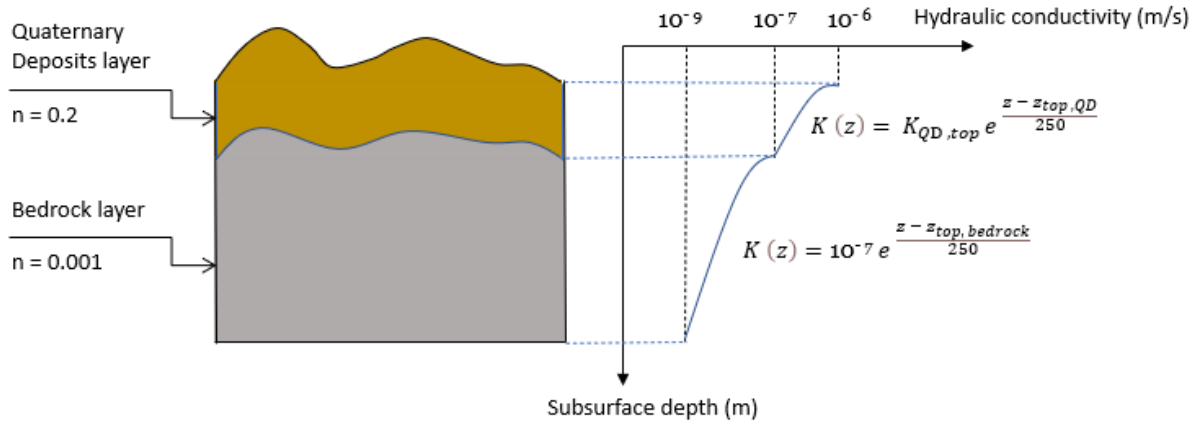

Figure 9 Illustration of the spatial variation of the hydraulic conductivity in the Quaternary deposits and the bedrock (figure modified after Mojarrad et al. (2021)).

4.1.2 Boundary conditions

The approach for the modeling was to assume a topography-controlled groundwater surface resulting in an entirely saturated domain. The top surface has a Dirichlet BC in discharge areas due to implementing a topography-controlled groundwater surface. In contrast, the recharge areas have a Neumann BC due to the mesh smoothing in these areas. The bottom of the bedrock domain was assigned a no-flow boundary, i.e., a variation of Neuman BC. The lateral boundaries were assigned a Dirichlet BC for the hydraulic head, controlled by the elevation of the surface topography.

4.1.3 Mesh in COMSOL Multiphysics

The finer the mesh that is used for the model, the more accurate solution can be obtained, this is especially true for larger models that require many elements in the mesh. Though, a finer mesh also requires larger RAM memory for the computation. The mesh of the model in COMSOL can either be built up using a pre-defined or user-defined mesh. The mesh size can be manually selected, it ranges from extremely coarse to extremely fine, where a finer mesh size can give a more accurate representation since the min element size is smaller.

The mesh for the model was built up using a user-defined mesh, which can reduce the computational time for models with many elements, and where the element types and sizes can be user-defined. Different types of meshes were applied with trial and error to try and accommodate for the limitation with computational cost. It was decided to go with a Swept mesh method for the soil domain and a Free Triangular mesh method for the bedrock domain with the reasoning that previous studies by Mojarrad et al. (2021) used these mesh methods for his model of Krycklan catchment in COMSOL.

Due to computational cost and the limitations with the RAM memory of the computer, the finest possible pre-defined mesh size in COMSOL was found to be *Finer* mesh which has a pre-defined min element size of 46.4 m. This min element size might not account for the resolution of the original 2 m topography DEM in the meshing of the model in COMSOL, thus, resulting in an additional type of mesh smoothing of the 2 m resolution. Due to this reason, it was decided that the element size parameters of

the mesh would instead be user-defined with reference to the resolution used in the mesh smoothing applied in the recharge areas. Meaning, if a mesh smoothing of 70 meters was applied, then the minimum element size was defined as 70 m and so on, except for the 2 m resolution due to the limitations earlier explained in this paragraph. Since the 2 m resolution might not be accurately accounted for by the min element size of the mesh in COMSOL, this method was applied to have a fairer comparison of the infiltration in recharge areas.

The built-in mesh sizes of COMSOL do not have a pre-defined option of a min element size of 40, 70, 84 or 120 m. Therefore, the mathematical relationships of the different element size parameters were found using the polynomial trendline tool of Excel, see Appendix 1 for the plots and trendlines of all the element parameters. The pre-defined element size parameters were plotted against a reference number, see table 2, and from this a reference number corresponding to the user-defined min element sizes was calculated with the polynomial equation for the min element size, see Figure 10 and table 3, which was used to calculate the other elements size parameters corresponding to that min element size by using their corresponding polynomial equation. These user-defined element parameters were then used in the mesh built of the domains. The min element size for the 2 m resolution DEM is 40 m, due to the limitations discussed above, and therefore has the corresponding element size parameters to that min element size.

Table 2 Reference number to each pre-defined mesh size in COMSOL and their corresponding pre-defined min element size.

Mesh size Pre-defined	Extremely Coarse	Extra Coarse	Coarser	Coarse	Normal	Fine	Finer	Extra Fine	Extremely Fine
Reference number	1	2	3	4	5	6	7	8	9
Min element size (m)	812	626	464	325	209	116	46.4	17.4	2.32

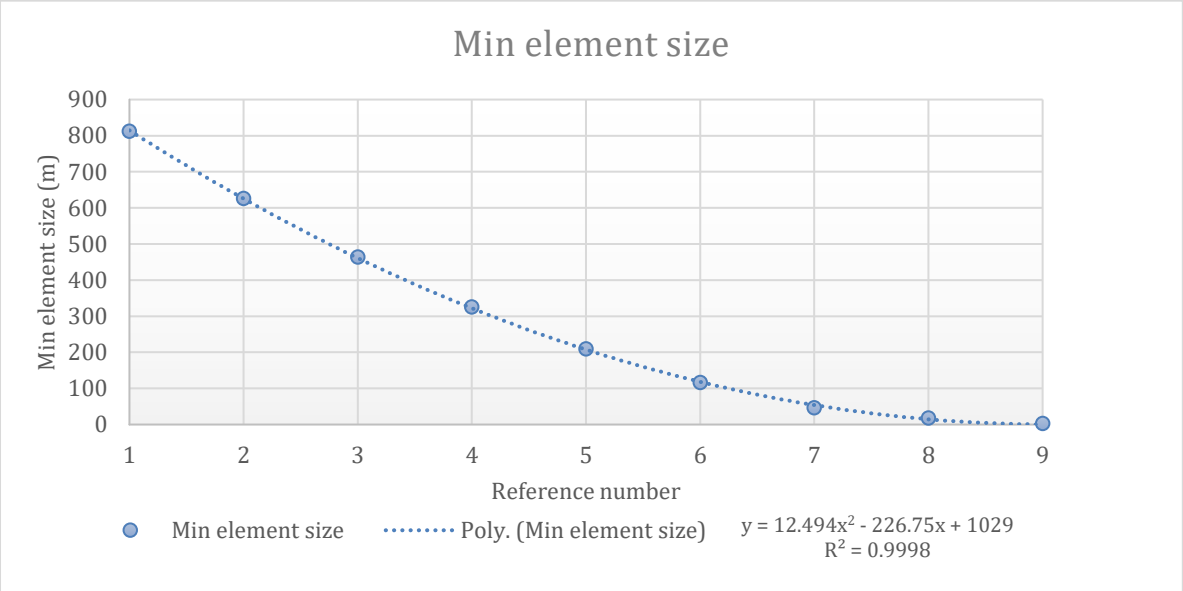

Figure 10 Pre-defined mesh size parameter min element size plotted against the reference number and its polynomial equation using trendline in Excel.

Table 3 Reference number to each user-defined min element size in COMSOL calculated from the polynomial equation in Figure 10 above. This reference value is used in the polynomial equation for the other element size parameters to calculate their corresponding value.

Min element size (m) User-defined	120	84	70	40
Reference number	5.98	6.48	6.71	7.29

4.2 Identification of recharge and discharge areas

The recharge and discharge areas of the catchment were identified through evaluation of the resulting vertical components of Darcy velocities at the top surface. A positive velocity entails an outflow of the domain, resulting in groundwater discharge. Conversely, a negative velocity entails an inflow to the domain, resulting in groundwater recharge. The vertical components of Darcy velocity values were imported as XY data in a .CSV file format into ArcMAP to identify these areas.

The Geometrical Interval classification method was used to evaluate the discharge flow distribution; this method is more suitable for skewed data, which is valid for the discharge values. The evapotranspiration discharge areas were identified by comparing the discharge flow distribution to the stream network in Krycklan Catchment; from this, a discharge threshold value was found for when the discharge is upheld by evapotranspiration or surface water flow. The area for each zone was approximated by the cell count and cell size for each raster layer.

The stream network was provided from previous studies by Mojarrad et al. (2021) and also created by using the hydrological tools in ArcMAP, where stream orders were applied with the method of Strahler (1957). The stream network, provided by Mojarrad et al. (2021), had been defined by setting a minimum width of 20 meters for the stream. Therefore, the minor tributaries might not be included in this stream network. The method developed by Strahler (1057) is suitable if both intermittent and permanent flow paths are on the designated map. This is since the first orders, the lowest ordered streams, are defined as the minor tributaries of the stream network, while the higher-ordered streams are the main streams of the stream network. Strahler's (1957) method uses the addition of stream orders, meaning that two first-order streams become one second-order stream – but two streams with different orders become the highest order out of the added streams.

4.2.1 Decrease of resolution in recharge areas

The purpose of decreasing the resolution in recharge areas is to achieve a modeled infiltration corresponding to the observed infiltration. Earlier studies by Mojarrad et al. (2021) have shown that the cell size, which gives a modeled infiltration corresponding to the observed, is 84 m. The cell sizes which were decided to be evaluated are 40, 70, 84, and 120 m to evaluate whether there is a convergence. The cubic convolution method was used as a resampling technique since it is suited for continuous data. To mosaic the recharge and discharge zones together, the cell size of the recharge zones was resampled to 2 m again but detaining the elevation values. The bedrock layer was also revised for each iteration to avoid intersections in COMSOL.

4.2.2 Landscape slope

The mean landscape slope was calculated using Zonal Statistics in ArcMAP and was evaluated for each iteration as the mesh smoothing had been applied to the topography. This was to assess whether the slope changes with a decreasing resolution since more minor undulations in the topography should be smoothed out.

4.2.3 Infiltration

The observed infiltration was calculated using SMHI: waterwebb (2020) water balance of the catchment, see Equation 4.2. Mean values are used for the whole catchment meaning there is steady states conditions, no temporal or spatial variations within the catchment of the infiltration.

$$I = P - ET = 734 - 349 = 385\,mm/yr \quad 4.2$$

5 Result

The result of the groundwater model computation is presented in this section. Mainly the result of using the original high-resolution 2 m DEM is presented, since the mesh smoothing was unsuccessful in decreasing the modelled infiltration and since the visual result is similar. The resolution used for each computation is presented as (*resolution in discharge areas*)x(*resolution in recharge areas*) in the following sections.

5.1 Landscape slope

The mean landscape slope of Krycklan catchment was calculated as the mean slope using the Zone Statistical tool in ArcMap, the result is presented in Figure 11 below. The slope decreases with decreasing resolution up to a certain cell size which for Krycklan catchment seems to be around 40 m. Smaller hills in the landscape have been found to have a steeper slope compared to large hills. Thus, indicating that microtopography and smaller undulations of the topography are smoothed when mesh smoothing is used. This is essentially the aim with applying mesh smoothing, since smaller undulations causes larger velocities, and therefore a larger infiltration.

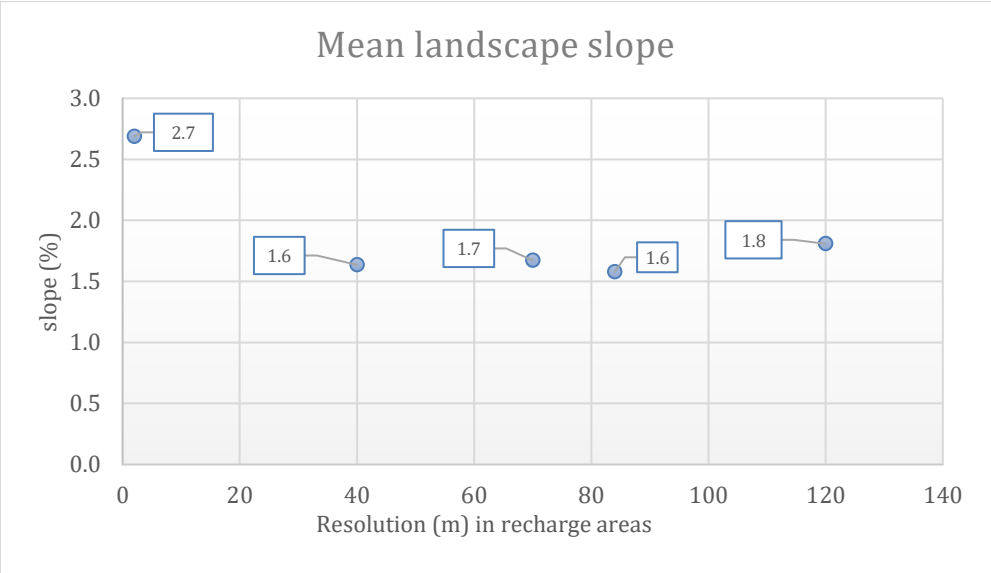

Figure 11 Mean landscape slope plotted for each iteration of mesh smoothing (original 2m, mesh smoothing in recharge areas; 40m, 70m, 84m & 120m).

5.2 Infiltration

The modelled infiltration in recharge areas of Krycklan catchment was estimated by evaluation of the negative vertical component of Darcy velocity at the top surface. These values were plotted using Boxplot and whiskers, see Figure 12, where the result is presented for the original 2 m resolution (with 40 m min element size in COMSOL due to limitations discussed under *4.1.3 Mesh in COMSOL*) and for when mesh smoothing has been applied to recharge areas of 40-, 70-, 84-, and 120 m (with the same min element size in COMSOL).

As can be observed in Figure 12, no decrease in the infiltration can be seen with decreasing resolution in the recharge areas, this is further discussed in 6. Discussion. The infiltration stays above 1000 mm/yr, which is much larger than the observed infiltration of 382 mm/yr in Krycklan catchment. The interquartile range does not have a significant variation between the different results when using a decrease of the resolution in recharge areas, the statistical dispersion therefore does not seem to change, and the distribution appears to be symmetric around the median value. There are many outliers for each result, outliers represent values at least 1.5 times larger than the interquartile range, where higher outlier values can be observed for when no mesh smoothing is applied in recharge areas (2 m resolution). The whiskers extend towards the minimum and maximum values, it can be observed that the minimum value does generally increase when applying mesh smoothing in recharge areas.

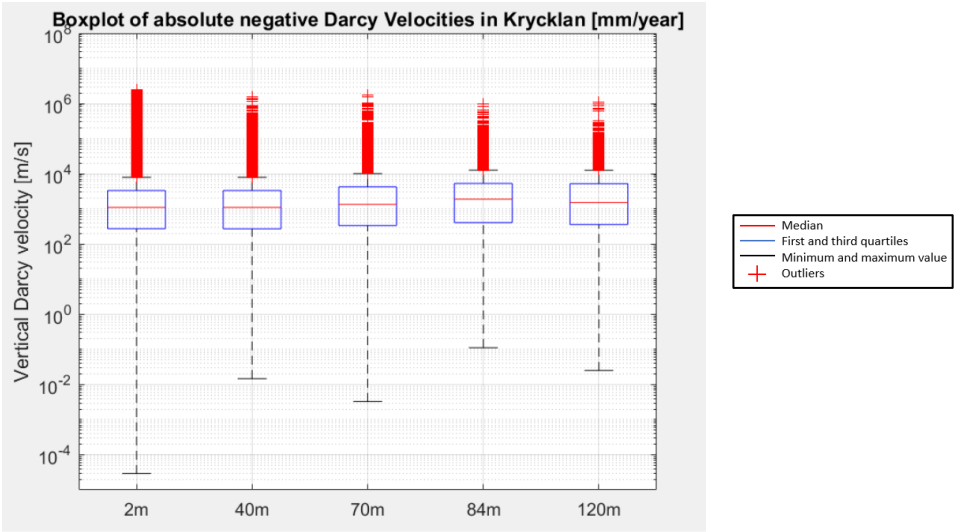

Figure 12 Boxplot with whiskers of the absolute negative Darcy velocities (mm/yr) at the top surface for the different resolutions applied in the mesh smoothing of the recharge areas.

5.3 Identification of recharge and discharge areas

The vertical component of Darcy velocity at the topography was imported into ArcMap and presented as a velocity range in the landscape of Krycklan catchment, see Figure 13 for result of the original 2 m DEM. The highest discharged values can be observed in the same locations as where data of the stream network is present. This can also be observed for the highest recharge values, indicating high recharge from water flow in streams. The recharge and discharge areas of Krycklan catchment was identified by evaluating the direction of the vertical component of Darcy velocities at the topography where a negative velocity indicates recharge and a positive velocity indicates discharge, see Figure 14 for illustration of the recharge and discharge areas for the original 2 m DEM. The range of Darcy velocity for when mesh smoothing has been applied in the recharge areas are presented in Appendix 2, and the corresponding identification of recharge and discharge areas are presented in Appendix 3.

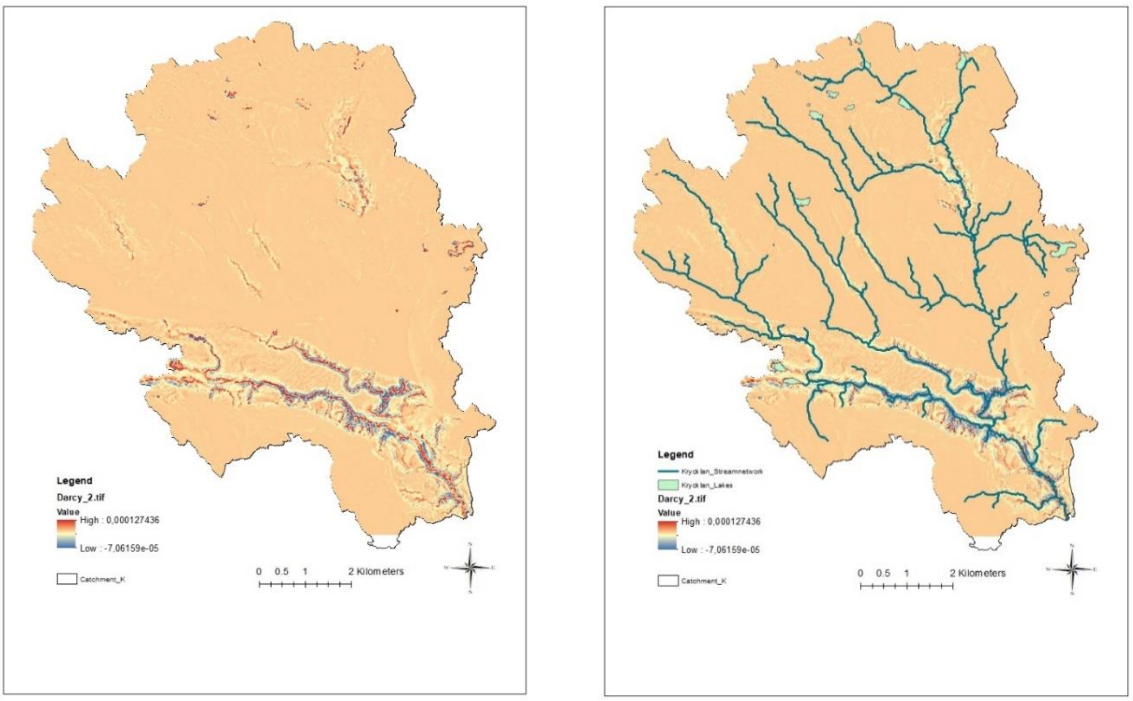

(a) (b)

Figure 13 Darcy velocity range in Krycklan illustrated using ArcMAP, resolution 2x2m. Without (a) and with (b) stream network and lakes (obtained from Mojarrad et al. (2021)) in Krycklan catchment.

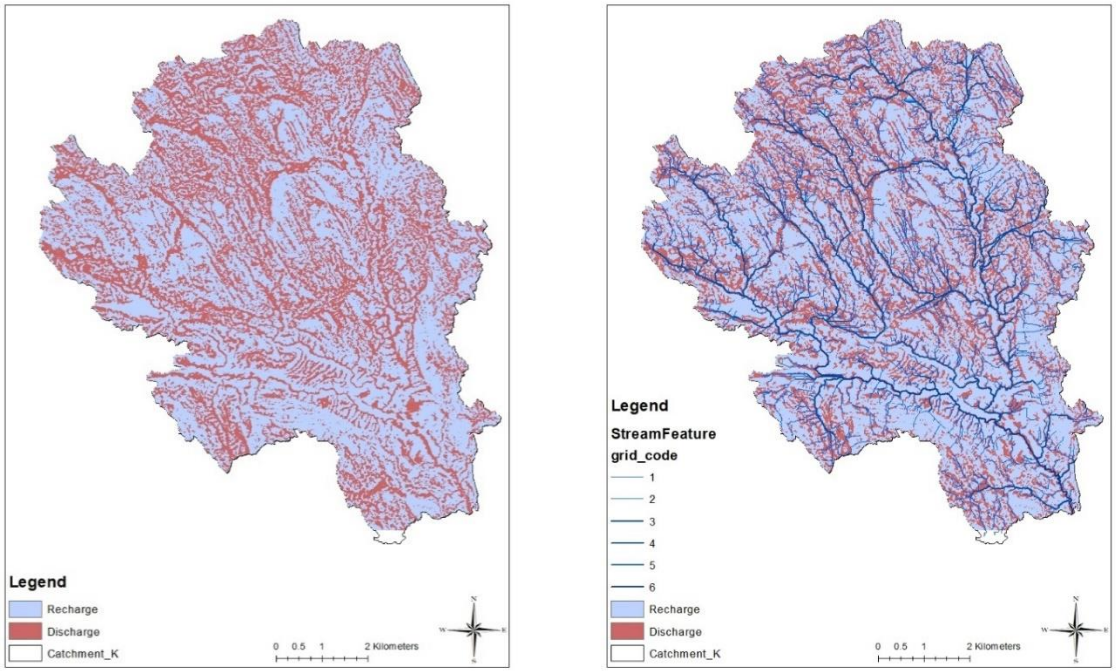

(a) (b)

Figure 14 Recharge and discharge areas in Krycklan illustrated using ArcMAP, resolution 2x2m. Without (a) and with (b) stream network and lakes in Krycklan catchment. The thinner blue lines represent the lower ordered streams (1 & 2). The stream network which was created with hydrological tools in ArcMAP is used in these illustrations.

5.4 Groundwater discharge flow distribution

The distribution of groundwater discharge values was evaluated for the negative Darcy velocities using the Geometrical Interval classification method in ArcMAP, the distribution is presented in Figure 15. The highest discharge values are observed in the same location as the main stream network, but lower values can be observed through the landscape. The distribution for when mesh smoothing has been applied in recharge areas are presented in Appendix 4.

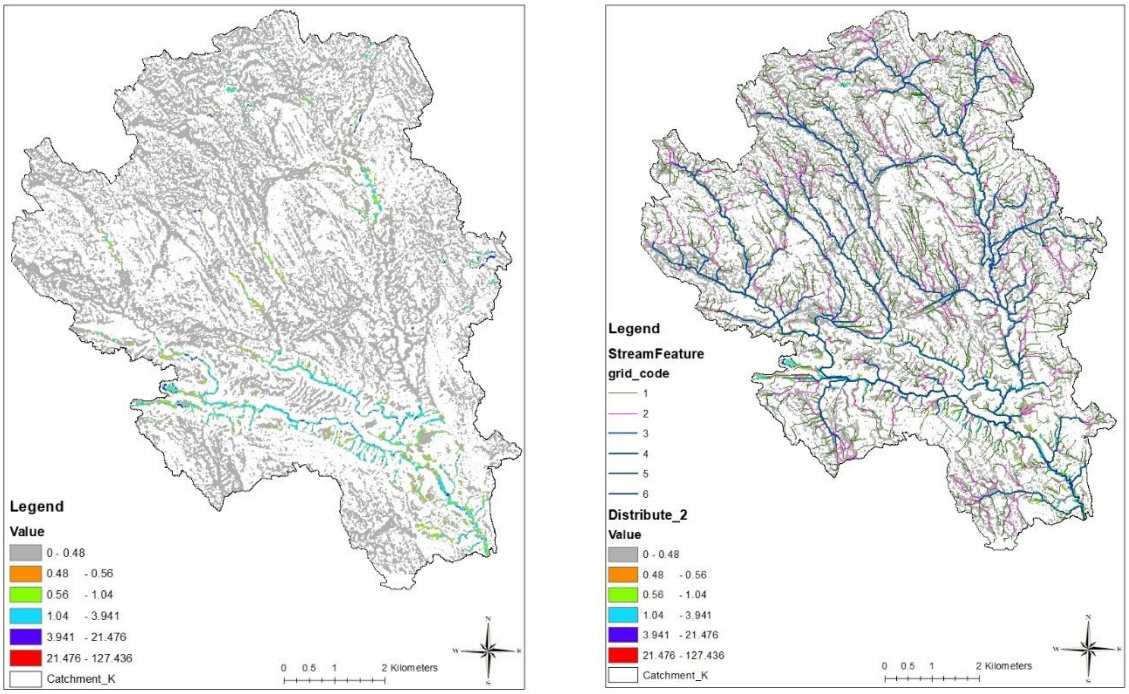

(a) (b)

Figure 15 Distribution of discharge values (10^{-6} m/s) in Krycklan, resolution 2x2m. Without (a) and with (b) stream network and lakes in Krycklan catchment. The two lower ordered streams are presented in green (1) and pink (2) for better visualization. The stream network which was created with hydrological tools in ArcMAP is used in these illustrations.

Smaller discharge values can be observed where no data of the stream network is present, and in some areas which appears to follow smaller tributaries of the stream network. This observation is presented in Figure 16, which illustrates a closer look for the comparison of the grey areas with lower discharge values and the stream network. As can be observed in Figure 16, on the left zoomed in figure, the grey areas do seem to follow smaller tributaries. While on the right zoomed in figure, the grey areas do not seem to follow smaller tributaries of the stream network. This kind of pattern is coherent throughout the landscape, indicating that some of the grey areas can potentially be areas where groundwater evapotranspiration is present.

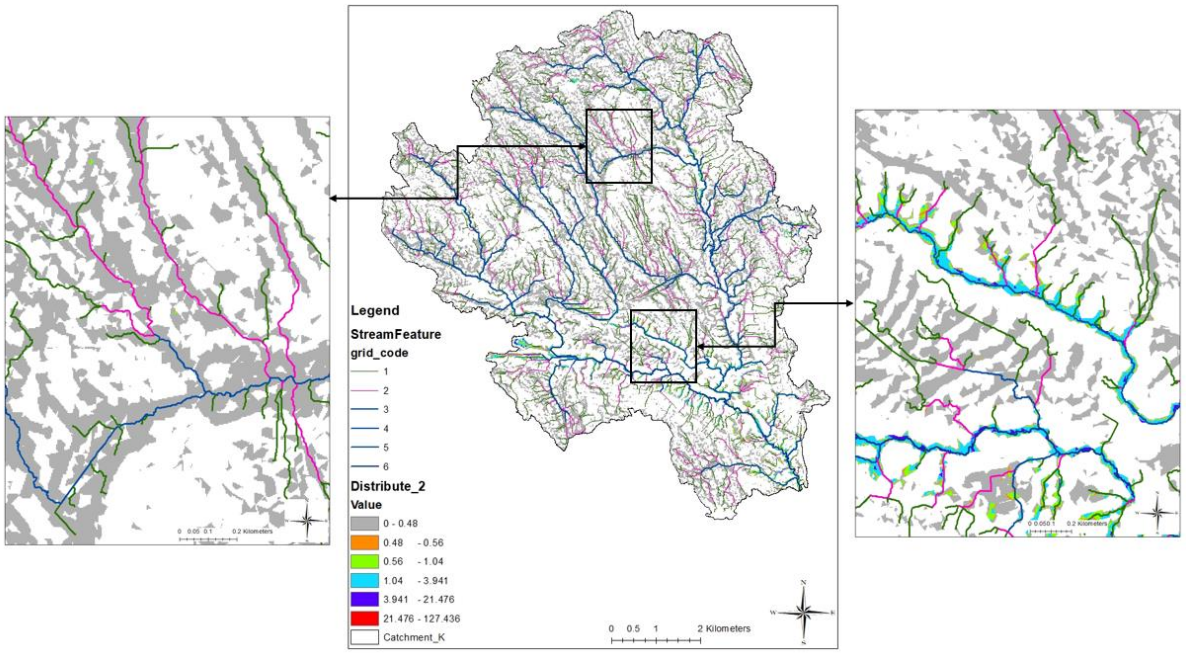

Figure 16 Distribution of discharge values (10-6 m/s) in Krycklan, resolution 2x2m. Close up showing comparison of the stream network and the flow distribution. The lower ordered streams are marked in green (1) and pink (2) to better separate them from higher ordered streams.

5.4.1 Threshold value

A threshold value for the discharge was determined by comparing the discharge distribution to the data for the extent of the stream network as present. This was to evaluate the distribution of the lower discharge values (the grey areas of Figure 15-16) observed in the catchment and which was assumed to represent areas where groundwater evapotranspiration potentially can be present. The threshold value (th. v) for each iteration of applying mesh smoothing in recharge areas is presented in Figure 17 below, where a decrease of the th. v generally can be observed.

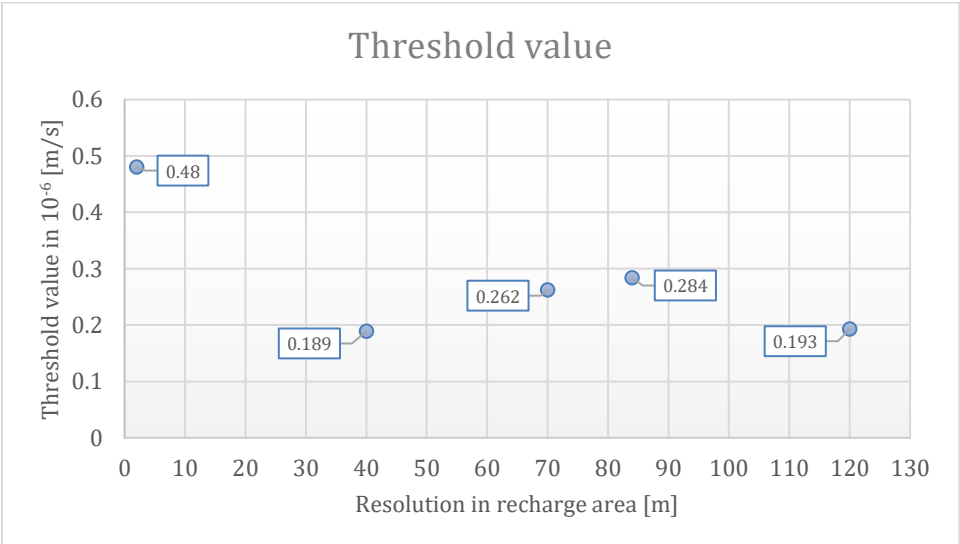

Figure 17 Plot of threshold values for the discharge flow of when the water balance is upheld by surface water discharge (velocities > th. v) or by evapotranspiration (velocities < th. v).

5.4.2 Areal distribution

The areal distribution between the areas where the water balance is assumed to be upheld by evapotranspiration (velocities < th. v) or by surface water flow (velocities > th. v) was evaluated by calculating total area of these areas. The areal distribution is presented in Figure 18, as well as a comparison of the area for each iteration with mesh smoothing of recharge areas. When evaluating this distribution, a critical component is to consider the accuracy of the th. v., as discharge values below the th. v could belong to areas where the water balance is upheld through discharge in surface water, as observed in Figure 16.

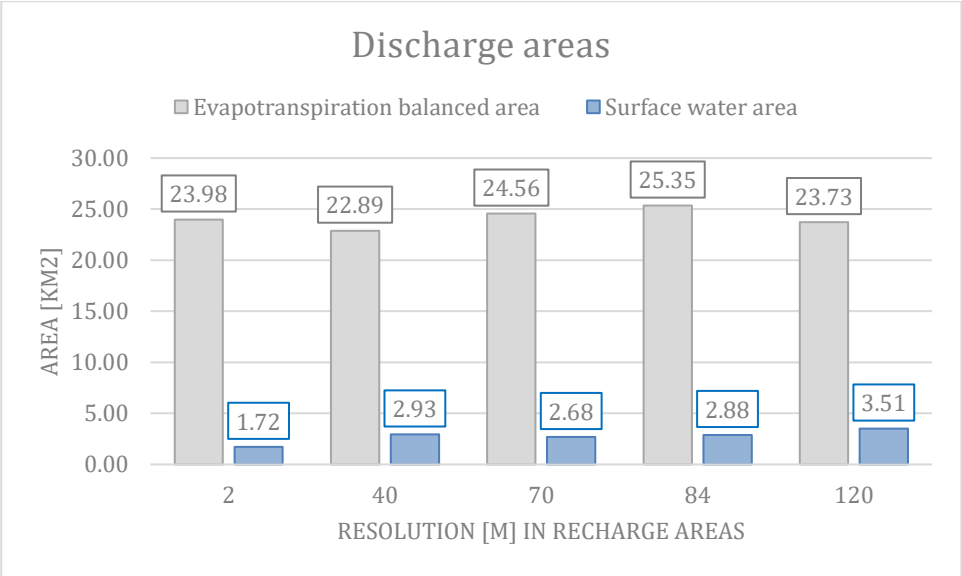

Figure 18 Presentation of the area for the evapotranspiration discharge area, and comparison between the different resolutions [m] in recharge areas.

5.4.3 Evapotranspiration discharge flow distribution

The areas where the water balance is assumed to be upheld by evapotranspiration was assumed to be where the discharge values are below the th. v and the distribution of these values is presented in Figure 19. The highest values are found near the stream network of Krycklan catchment. This could indicate presence of higher groundwater evapotranspiration in the riparian zones of the landscape. Again, a critical component is to consider the accuracy of the th. v. when evaluating this distribution, as discharge values below the th. v could belong to areas where the water balance is upheld through surface water, as observed in Figure 16. This does however present the distribution of the lower discharge values of Krycklan catchment. The distribution for when mesh smoothing has been applied in recharge areas are presented in Appendix 5.

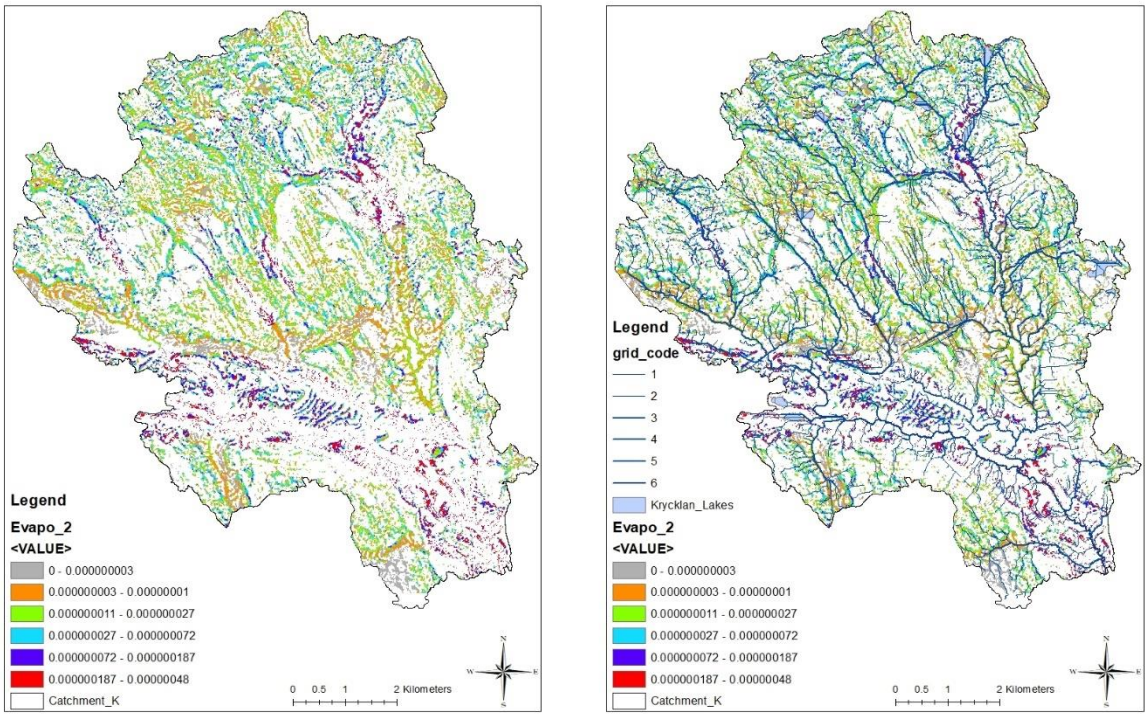

(a) (b)

Figure 19 Distribution of evapotranspiration discharge values in Krycklan, resolution 2x2m. Without (a) and with (b) stream network and lakes in Krycklan catchment. the stream network which was created with hydrological tools in ArcMAP is used in these illustrations.

6 Discussion

This section presents a discussion of the result, uncertainties of the model and data, and recommendations for future studies.

6.1 Discharge and recharge areas

Identifying discharge and recharge areas in Krycklan Catchment by distinguishing between the positive and negative resulting Darcy velocities from the computation in COMSOL was successful. The accuracy of these values depends on several factors, although for most, on the model's capability of predicting the groundwater flow pattern of Krycklan catchment. To evaluate this, the distribution of the negative Darcy velocities was compared to data of surface water bodies. This showed that the location of higher negative velocities corresponded to the location of the stream network, showing a relatively accurate prediction of the groundwater flow pattern. The groundwater discharge distribution showed that there was groundwater discharge were no data of surface water bodies were present. In these areas, the water balance was assumed as upheld by evapotranspiration, and these areas were found throughout the landscape. Krycklan catchment is defined as a forested catchment that, compared to grassland catchments, has higher evapotranspiration values; this makes it reasonable that there could be a large extent of evapotranspiration balanced discharge areas in Krycklan catchment.

6.1.1 Threshold value and evapotranspiration balanced discharge areas

The threshold value for when the water balance is upheld through evapotranspiration or surface flow was determined by comparing the distribution of discharge values to data of surface water bodies. This value is not certain but was used for an approximate determination. The areal distribution between areas where the water balance is upheld through evapotranspiration or by surface water flow, is highly dependent on the accuracy of the threshold value. Also, discharge values below the threshold value could be observed in locations where the stream network was present, indicating that the accuracy of the threshold value is not very high. Thus, the areal distribution is not very accurate. However, the evapotranspiration distribution showed higher discharge flow rates near surface waters. This is a relatively accurate prediction of the groundwater flow pattern since it has been shown that riparian areas have a higher evapotranspiration rate than the rest of a catchment. Denser vegetation covers naturally form near water sources, such as surface water bodies, resulting in higher evapotranspiration in these areas.

The analysis in ArcMAP of the discharge flow distribution showed reaches of the river, which had a discharge flow value lower than the threshold value. A low discharge velocity in stream locations can be due to low flow velocities in streams or groundwater gaining and losing reaches of the stream (i.e., recharge and discharge of groundwater). The evaluation of discharge distribution in evapotranspiration balanced areas, therefore, included discharge values that should have been identified as surface flow discharge. The magnitude of discharge velocities in evapotranspiration areas might be lower, and the distribution itself could also be different. The actual evapotranspiration rate is dependent on several factors, not only the groundwater discharge. The water that vegetation can adsorb is not only from groundwater discharge but also from soil moisture, stored water in the plant itself, and atmospheric humidification. If the actual evapotranspiration rate is to be considered, then the evapotranspiration in recharge areas must also be accounted for. Other factors that need to be considered are solar radiation, wind velocity, and plant species, which affect the evapotranspiration rate.

A flatter topography characterizes the downstream regions of Krycklan catchment compared to the upstream regions. The soil depths are also greater, and there is presence of soil layers with higher hydraulic conductivities. This is reflected in the discharge flow distribution presented in the result, with higher discharge velocities in the downstream regions. Mojarrad et al. (2021) identified deep groundwater discharge points in the catchment; these were in the stream network and lakes with a higher frequency in the downstream region. These locations correspond well to the locations in which the highest discharge velocities were observed in the discharge flow distribution of this thesis. This thesis showed discharge zones throughout the catchment; comparing this to the result of Mojarrad et al. (2021), the evapotranspiration discharge areas could be discharge points for local or intermediate groundwater flow.

The stream network, which was created using the hydrological tools in ArcMAP, shows that the areas assumed to be discharge areas where the water balance is upheld by evapotranspiration might instead be areas where the discharge is upheld by surface water flow. This could be either smaller tributaries or temporary smaller streams that come forward during the spring or fall. This makes the definition of the threshold value used in this study problematic, both since there can be a temporal variation and since the distribution of the discharge values does not seem to account for these smaller streams in the landscape.

The result of this studies corresponds with the result of Tsang et al. (2014), that the groundwater evapotranspiration is higher in flatter topography areas. The result of this study showed that the total area of evapotranspiration discharge areas is approximately 35 % of the total catchment area, while Tsang et al. (2014) found an area of 10 %. This also indicates that a more accurately defined discharge

threshold value is important. Since this model assumes a shallow groundwater surface throughout the whole domain, more specifically that the groundwater surface follows that topography, it is harder to determine whether the distribution of groundwater evapotranspiration correlates more to areas with shallow groundwater or dense vegetative surface. Although, the distribution does show a higher groundwater evapotranspiration in flatter topography and near surface water bodies, i.e., presumable in riparian zones. Comparing the groundwater discharge distribution in evapotranspiration balanced areas with the tree volume map (see figure 5), there is not a clear correlation between the areas with denser tree volume and areas with higher evapotranspiration discharge values. This could be due to an inaccurate illustration of the evapotranspiration distribution since some of the velocity values could in fact belong to discharge through surface water flow. However, the discharge is lower in areas where there are fields, compared to areas where there are trees.

6.2 Data uncertainties

There can always be inaccuracies in data, whether it is elevation data, hydraulic conductivity values, or hydrological data. The importance of accuracy of data is also dependent on the purpose. Both elevation data and hydraulic conductivity are governing factors of the groundwater flow pattern; the accuracy of these data is, therefore, essential for this thesis. The accuracy of elevation data depends on the resolution, where a higher resolution can account for more minor undulations in the topography. When applying a decreased resolution in recharge areas, these more minor undulations are smoothed, decreasing the accuracy. This is, however, the purpose of implementing mesh smoothing of the topography in this thesis.

The hydraulic conductivities used for this thesis were the values used by Mojarrad et al. (2021) in his doctoral thesis, where he modeled Krycklan catchment similarly using COMSOL. The hydraulic conductivity of different soil layers usually varies depending on the deposition and other factors; till especially has a wide range of hydraulic conductivities, and it is difficult to depict the conditions accurately. Compared to this thesis, the model by Mojarrad et al. (2021) had different stratification and hydraulic conductivities. At the top boundary, he had an additional soil layer, a sediment layer, which inhabits different hydraulic conductivities. This could result in differences in the infiltration values between our models. The same exponential decay expression for the hydraulic conductivity of the Quaternary deposits and the bedrock was used; therefore, it should not be causing a different result. Another difference could be the mean landscape slope which affects the infiltration.

6.3 Model uncertainties

The accuracy of the geometry built in COMSOL is highly affected by the mesh element size. A domain with thin regions requires a finer mesh element size to avoid intersections and have an accurate account of these regions. The soil domain had several thin regions and more minor undulations in the topography due to the high-resolution DEM, which was used as the original topography file and in discharge areas for each iteration, had a resolution of 2x2m. This would require a minimum element size of around 2m which was impossible due to computational cost. The minimum element size ended up being 46.4 m, which affects the accuracy of the geometry build and, in return, the accuracy of the model's groundwater flow prediction. This also resulted in a mesh smoothing of the 2x2m resolution DEM file before the mesh smoothing was applied in ArcMAP, which means that the discharge areas were constantly subjected to mesh smoothing in COMSOL. This is seen in the infiltration values of the recharge area where a 2x2m resolution gave an infiltration of 1099mm/yr, which is much lower compared to the result of Mojarrad et al. (2021). He succeeded in applying a minimum element mesh size of 2 m for the topography in COMSOL, which could account for the 2x2m resolution DEM. He also

used the third layer on top of the Quaternary deposits, a sediment layer, which affects the infiltration value due to different properties such as the hydraulic conductivity.

A topography-controlled groundwater surface was successfully implemented in COMSOL; this was confirmed in the result by verifying that the hydraulic head was equal to the elevation. The application of a topography-controlled groundwater surface in groundwater modeling results in a soil domain that is completely saturated. This is often not the case in reality, and this does result in a modeled infiltration that is greater than the observed infiltration. A method to solve this is to implement mesh smoothing in recharge areas, although for this study, the mesh smoothing was unsuccessful in lowering the infiltration. The magnitude of the modeled infiltration is larger than the observed one in Krycklan catchment; this both affects the distribution of the discharge values and the magnitude of the discharge values. An accurate infiltration value would change the outcome.

6.4 Recommendations for future studies

In this study, mean annual data values are used. This implies steady state conditions, and therefore no temporal variations have been evaluated. Reasonable, there is a temporal variation of both the infiltration, groundwater recharge, and discharge. Especially considering that the precipitation itself has a temporal variation which is the water source for groundwater recharge and considering the delay of groundwater recharge in the winter until snowmelt and frozen land which would affect the water balance of the catchment if a temporal variation were to be introduced. Also considering that the evapotranspiration certainly has a temporal variation, this could be even more substantial in humid boreal regions, due to lower groundwater evapotranspiration during winter months. In Nothern Sweden it is not uncommon with flooded land during the spring flood, caused by the combination of precipitation and snowmelt, which can fill up temporal tributaries of the stream network and increase the areal extent of rivers and lakes. There is also the temporal variation between different years, and climate change which can affect the hydrological conditions in the future that can be important to evaluate.

This thesis has not evaluated the evapotranspiration rate; instead, the groundwater discharge in evapotranspiration balanced areas. This could be further evaluated for future studies, where factors such as plant species, solar radiation, soil humidity, atmospheric humidification, and wind velocity can be accounted for. Also, this study has not evaluated particle tracing with groundwater flow. This could be important to further evaluate contaminant transport with groundwater flow to evapotranspiration balanced discharge areas and evaluate if these areas are discharge zones for mainly local, intermediate, or regional groundwater flow.

7 Conclusion

This thesis aimed to evaluate the groundwater discharge distribution of Krycklan. A groundwater model was built in COMSOL Multiphysics using high-resolution DEM and hydrogeological boundary conditions. A topography-controlled groundwater surface for the top boundary conditions was successfully modeled; however, the magnitude of the modeled infiltration was higher than the observed infiltration and it could not be successfully lowered by decreasing the resolution in recharge areas. Thus, the model could not be validated with reference to the observed infiltration in Krycklan catchment. However, the result showed accuracy in the models' capability to predict the groundwater flow pattern. Negative Darcy velocities were observed in locations where data on surface water exists, and the highest discharge values were also observed in the same locations.

The discharge and recharge areas of Krycklan catchment could be identified with reference to the direction of the vertical component of Darcy velocity at the top surface. The distribution of the groundwater discharge showed indications of discharge areas where the water balance was upheld by evapotranspiration and upheld by surface water flow. A discharge threshold value for the distinction of these areas was assumed with reference to surface water data compared to the discharge distribution. The discharge distribution in evapotranspiration balanced areas was also evaluated, indicating a higher discharge near surface waters.

The result of this thesis shows an interesting distribution of the discharge areas, with presence of evapotranspiration balanced areas. For contaminant transport and safety assessment of high nuclear waste storage facilities, a model or method which could assess this issue would be important. Further studies on the subject have been suggested, as the result of this thesis is dependent on an inaccurate modeled infiltration and several simplifications such as the discharge threshold value defined only by comparing the discharge flow distribution to the main streams and no temporal variation.

8 References

Arnold, J.G. & Allen, P.M. 1996. Estimating hydrologic budgets for three Illinois watersheds. Journal of Hydrology 176: 57–77. DOI: 10.1016/0022-1694(95)02782-3.

Atangana, A. 2018. Chapter 2 - Principle of Groundwater Flow. Fractional Operators with Constant and Variable Order with Application to Geo-Hydrology. Academic Press. 2018. Pages 15-47. ISBN 9780128096703. https://doi.org/10.1016/B978-0-12-809670-3.00002-3.

Chow, V., Maidment, D. and Mays, L. 1988. Applied Hydrology. McGraw-Hill Boo Company, New York.

Condon, L. and Maxwell, R. 2015. Evaluating the relationship between topography and groundwater using outputs from a continental-scale integrated hydrology model. Water Resources Research. 51. 10.1002/2014WR016774.

de Lange, W-J. 1999. A Cauchy boundary condition for the lumped interaction between an arbitrary number of surface waters and a regional aquifer. Journal of Hydrology. Volume 226. Issues 3–4. 1999. Pages 250-261. ISSN 0022-1694. https://doi.org/10.1016/S0022-1694(99)00143-2

Doble, R. and Crosbie, R. 2016. Review: Current and emerging methods for catchment-scale modelling of recharge and evapotranspiration from shallow groundwater. Hydrogeology Journal. 25. 10.1007/s10040-016-1470-3.

Erdbrügger, J. van Meerveld, I. Bishop, K. and Seibert, J. 2021a. Effect of DEM-smoothing and -aggregation on topographically-based flow directions and catchment boundaries, J. Hydrol., 602(November 2020), 126717, doi:10.1016/j.jhydrol.2021.126717, 2021 .

Erdbrügger, J. van Meerveld, I. Seibert, J. and Bishop, K. 2021b. Flow directions of shallow groundwater in a boreal catchment. EGU General Assembly 2021, 19–30 Apr 2021, EGU21-9384, https://doi.org/10.5194/egusphere-egu21-9384, 2021

Espeby, B. and Gustafsson, J. P., 1998. Vatten och ämnestransport i den omättade zonen. TRITA-AMI Rapport 3038. Avdelningen för mark- och vattenresurser; institutionen för anläggning och miljö. KTH Royal Institute of Technology.

Fitts, R-C. 2013. 2 - Physical Properties, Editor(s): Charles R. Fitts, Groundwater Science (Second Edition), Academic Press, 2013, Pages 23-45, ISBN 9780123847058, https://doi.org/10.1016/B978-0-12-384705-8.00002-9

Freeze, A. & Cherry, J. 1979. Groundwater: Englewood Cliffs. In: New Jersey. http://hydrogeologistswithoutborders.org/wordpress/1979-english/

Groeneveld, D., Baugh, W., Sanderson, J. and Cooper, D. 2007. Annual Groundwater Evapotranspiration Mapped from Single Satellite Scenes. Journal of Hydrology - J HYDROL. 344. 146-156. 10.1016/j.jhydrol.2007.07.002.

Hajitema, H. M. and S. Mitchell-Bruker. 2005. Are water tables a subdued replica of the topography?, Ground Water, [publication]. 43, 781–786. https://doi.org/10.1111/j.1745-6584.2005.00090.x

Hedberg, S. & Svensson, T. 2016. Våtmarksutredning Anläggande av stolpfundament sträckan Långbjörn - Storfinnforsen. Geosigma AB. Uppdragsnr. 604359. Grap 16189.

https://www.svk.se/contentassets/708910e9c7a343538e21b087c6ebe37c/bilaga-6-vatmarksutredning.pdf

Hjerne, C., Thorsbrink, M., Thunholm, B., Andersson, J. & Dahlqvist, P. 2021. Hydraulisk konduktivitet i Sveriges berggrund. SGU-report 2021:09. https://resource.sgu.se/dokument/publikation/sgurapport/sgurapport202109rapport/s2109-rapport.pdf

Jayakody, P., Parajuli, P.B., Sassenrath, G.F. and Ouyang, Y. (2014), Relationships Between Water Table and Model Simulated ET. Groundwater, 52: 303-310. https://doi.org/10.1111/gwat.12053

Jazayeri, A. and Werner, A.D. (2019), Boundary Condition Nomenclature Confusion in Groundwater Flow Modeling. Groundwater, 57: 664-668. https://doi.org/10.1111/gwat.12893

Kurc, S. and Small, E. 2004. Dynamics of evapotranspiration in semiarid grassland and shrubland ecosystems during the summer monsoon season, central New Mexico. Water Resources. Res., 40: 1–15

Lantmäteriet: Min karta. 2022. Accessed via: https://minkarta.lantmateriet.se/ [last visited 2022-02-15]

Laudon, H., Taberman, I., Ågren, A., Futter, M., Ottosson-Lofvenius, M., Bishop, K., 2013. The Krycklan Catchment Study - A flagship infrastructure for hydrology, biogeochemistry, and climate research in the boreal landscape. Water Resources. Res. 49, 7154–7158. https://doi.org/10.1002/wrcr.20520.

Leach, J.A., Lidberg, W., Kuglerov, L., Peralta-Tapia, A., Ågren, A., Laudon, H., 2017. Evaluating topography-based predictions of shallow lateral groundwater discharge zones for a boreal lake-stream system. Water Resources. Res. 53, 5420–5437. https:// doi.org/10.1002/2016WR019804.Received.

Lee, C.H. 1912. Water resources of a part of Owens Valley. California: U.S. Geological Survey Water-Supply. Paper 294.

Levine, J.B. & Salvucci, G.D. 1999. Equilibrium analysis of groundwater-vadose zone interactions and the resulting spatial distribution of hydrologic fluxes across a Canadian Prairie. Water Resources Research 35: 1369–1383. DOI: 10.1029/1999wr900018.

Lidberg, W, Nilsson, M, Lundmark, T, Ågren, AM. 2017. Evaluating preprocessing methods of digital elevation models for hydrological modelling. Hydrological Processes. 2017; 31: 4660– 4668. https://doi.org/10.1002/hyp.11385

Lind, B. & Nyborg, M. (1986). Moränstruktur och hydraulisk konduktivitet. The influence of sediment structures on hydraulic conductivity in till - progress report. Meddelande nr.8. Göteborg 1986. Chalmers Tekniska Högskola; Geohydrologiska forskningsgruppen; Geologi; Geoteknik med grundliggning; Vattenbyggnad; Vattenförsörjnings· och avloppsteknik. ISSN 0347 - 8165. Accessed via: https://publications.lib.chalmers.se/records/fulltext/179514/local_179514.pdf

Lyon, S.W., Nathanson, M., Spans, A., Grabs, T., Laudon, H., Temnerud, J., Bishop, K.H., Seibert, J., 2012. Specific discharge variability in a boreal landscape. Water Resources. Res. 48, 1–13. https://doi.org/10.1029/2011WR011073

Marklund, L. & Wörman, A. 2011. The use of spectral analysis-based exact solutions to characterize topography-controlled groundwater flow. Hydrogeology Journal: Official Journal of the International

Association of Hydrogeologists. Volume 19; Number 8. ISSN 1431-2174. Hydrogeol J (2011) 19:1531-1543. DOI: 10.1007/s10040-011-0768-4

Marklund, L. 2009. Topographic Control of Groundwater Flow, KTH. TRITA-LWR PhD Thesis 1052.

Meinzer, O.E. 1917. Geology and water resources of Big Smoky, Clayton, and Alkali Springs Valleys. Nevada: U.S. Geological Survey Water-Supply. Paper 423.

Mojarrad, B-B., Riml, J., Wörman, A., & Laudon, H. (2019). Fragmentation of the hyporheic zone due to regional groundwater circulation. Water Resources Research, 55, 1242– 1262. https://doi.org/10.1029/2018WR024609

Mojarrad, B-B., Wörman, A., Riml, J. & Xu, S. 2021. Multi-Scale Surface Water-Groundwater Interaction: Implications for Groundwater Discharge Patterns. Doctoral Thesis in Resources, Energy and Infrastructure. TRITA-ABE-DLT-2138. KTH.

Nachabe, M., Shah, N., Ross, M. and Vomacka, J. (2005), Evapotranspiration of Two Vegetation Covers in a Shallow Water Table Environment. Soil Sci. Soc. Am. J., 69: 492-499. https://doi.org/10.2136/sssaj2005.0492

Nichols, W.D. 1992a. Energy budgets and resistance to energy transport in sparsely vegetated rangeland: Agricultural and Forest Meteorology. v. 60. p. 221-247.

Nichols, W.D. 1992b. The uncertainty of water budget estimates in the Great Basin, in Herrmann, R. ed. Managing water resources during global change: American Water Resources Association 28th Annual Conference and Symposium, Reno, Nev., Nov. 1-5, 1992, p. 309-317.

Nichols, W.D. 1993. Estimating discharge of shallow groundwater by transpiration from greasewood in the northern Great Basin: Water Resources Research. v. 29. no. 8. p. 2771- 2778.

Nichols, W.D. 1994. Groundwater discharge by phreatophyte shrubs in the Great Basin as related to the depth to groundwater: Water Resources Research. v. 30. no. 12. p. 3265-3274.

Nichols, W.D. 2000b. Chapter A. Determining Ground-Water Evapotranspiration From Phreatophyte Shrubs and Grasses as a Function of Plant Cover or Depth to Ground Water, Great Basin, Nevada and Eastern California in: Regional Ground-Water Evapotranspiration and Ground-Water Budgets, Great Basin, Nevada. 2000: U.S. Geological Survey Professional Paper: 1628

Nichols, W.D. 2000b. Chapter C. Regional Ground-Water Budgets and Ground-Water Flow, Eastern Nevada in: Regional Ground-Water Evapotranspiration and Ground-Water Budgets, Great Basin, Nevada. 2000: U.S. Geological Survey Professional Paper: 1628

Nichols, W.D., Laczniak, R.J., DeMeo, G.A., and Rapp, T.R. 1997. Estimated ground-water discharge by evapotranspiration, Ash Meadows National Wildlife Refuge. Nye County. Nevada. 1994: U.S. Geological Survey Water-Resources Investigations Report 97-4025. 13 p.

Ploum, S.W., Laudon, H., Peralta-tapia, A., Kuglerov´ a, L., 2020. Are dissolved organic carbon concentrations in riparian groundwater linked to hydrological pathways in the boreal forest ? Hydrol. Earth Syst. Sci. 24, 1709–1720

Rodhe, A., Seibert, J., 2011. Groundwater dynamics in a till hillslope: Flow directions, gradients and delay. Hydrol. Process. 25, 1899–1909. https://doi.org/10.1002/hyp.7946

Saar, MO. & Manga, M. 2004. Depth dependence of permeability in the Oregon cascades inferred from hydrogeologic, thermal, seismic, and magmatic modeling constraints. J Geophys Res Solid Earth 109(B4), B04204. doi:10.1029/2003JB002855

Satchithanantham, S., Wilson, F.H. and Glenn, J.A. 2017. Contrasting patterns of groundwater evapotranspiration in grass and tree dominated riparian zones of a temperate agricultural catchment. Journal of Hydrology. Volume 549. 2017. Pages 654-666. ISSN 0022-1694. https://doi.org/10.1016/j.jhydrol.2017.04.016.

Seibert, J., Bishop, K., Rodhe, A., McDonnell, J.J., 2003. Groundwater dynamics along a hillslope: A test of the steady state hypothesis. Water Resour. Res. 39, 1–9. https://doi.org/10.1029/2002WR001404

Shah, N., Nachabe, M. and Ross, M. 2007. Extinction Depth and Evapotranspiration from Ground Water under Selected Land Covers. Groundwater, 45: 329-338. https://doi.org/10.1111/j.1745-6584.2007.00302.x

SLU, 2010. SLU Skogskarta. Reached via: https://www.slu.se/centrumbildningar-och-projekt/riksskogstaxeringen/statistik-om-skog/slu-skogskarta/ [Last visited: 2022-06-04]

SMHI, n.d. Månads-, årstids- och årskartor. Reached via: https://www.smhi.se/data/meteorologi/kartor/normal/arsnederbord-normal [Last visited: 2022-06-14]

SMHI: Waterwebb, 2020. Modelldata per område (eng: Modeldata per area). Accessed via: https://vattenwebb.smhi.se/modelarea/ [Last visited: 2022-03-10]

Strahler, A.N. 1957. Quantitative analysis of watershed geomorphology. Transactions, American Geophysical Union 38:913–920.

Tabacchi, E., Lambs, L., Guilloy, H., Planty-Tabacchi, A-M., Muller, E. & Decamps, H. (2000). Impacts of Riparian Vegetation on Hydrological Processes. Hydrological Processes. vol. 14. 2959-2976. doi: 10.1002/1099-1085(200011/12)14:16/173.3.CO;2-2.

Tóth, J. (1963), A theoretical analysis of groundwater flow in small drainage basins, J. Geophys. Res., 68(16), 4795– 4812, doi:10.1029/JZ068i016p04795. https://doi.org/10.1029/JZ068i016p04795

Tóth, J. 1970. A conceptual model of the groundwater regime and the hydrogeologic environment, Journal of Hydrology, Volume 10, Issue 2, 1970, Pages 164-176, ISSN 0022-1694, https://doi.org/10.1016/0022-1694(70)90186-1

Tóth, J. 1999. Groundwater as a geologic agent: An overview of the causes, processes, and manifestations. Hydrogeology Journal 7, 1–14 (1999). https://doi.org/10.1007/s100400050176

Tsang, Y.-P., Hornberger, G., Kaplan, L.A., Newbold, J.D. and Aufdenkampe, A.K. 2014. A variable source area for groundwater evapotranspiration: impacts on modeling stream flow. Hydrol. Process., 28: 2439-2450. https://doi.org/10.1002/hyp.9811

White, W.N. 1932. A method of estimating ground-water supplies based on discharge by plants and evaporation from soil: Results of investigation in Escalante Valley, Utah. In Contributions to the hydrology of the United States 1932: U.S. Geological Survey Water-Supply Paper 659-A. USGS, Reston, VA.

Wörman, A. 2021. Master thesis meeting 2021-11-29. [personal communication].

Zhang, L., Dawes, W. R., and Walker, G. R. (2001), Response of mean annual evapotranspiration to vegetation changes at catchment scale, Water Resour. Res., 37(3), 701– 708, doi:10.1029/2000WR900325.

Zhang, L., Hickel, K., Dawes, W. R., Chiew, F. H. S., Western, A. W., and Briggs, P. R. (2004), A rational function approach for estimating mean annual evapotranspiration, Water Resour. Res., 40, W02502, doi:10.1029/2003WR002710.

9 Appendices

9.1 Appendix 1: Mathematical relationship of mesh element size parameters

Below are the reference number to each corresponding pre-defined mesh sizes in COMSOL and the plots of the mesh element size parameters, and their polynomial trendline from the trendline option in Excel, is presented.

Table 9.1.1 Reference number to each pre-defined mesh size in COMSOL and their corresponding pre-defined min element size.

Mesh size Pre-defined	Extremely Coarse	Extra Coarse	Coarser	Coarse	Normal	Fine	Finer	Extra Fine	Extremely Fine
Reference number	1	2	3	4	5	6	7	8	9

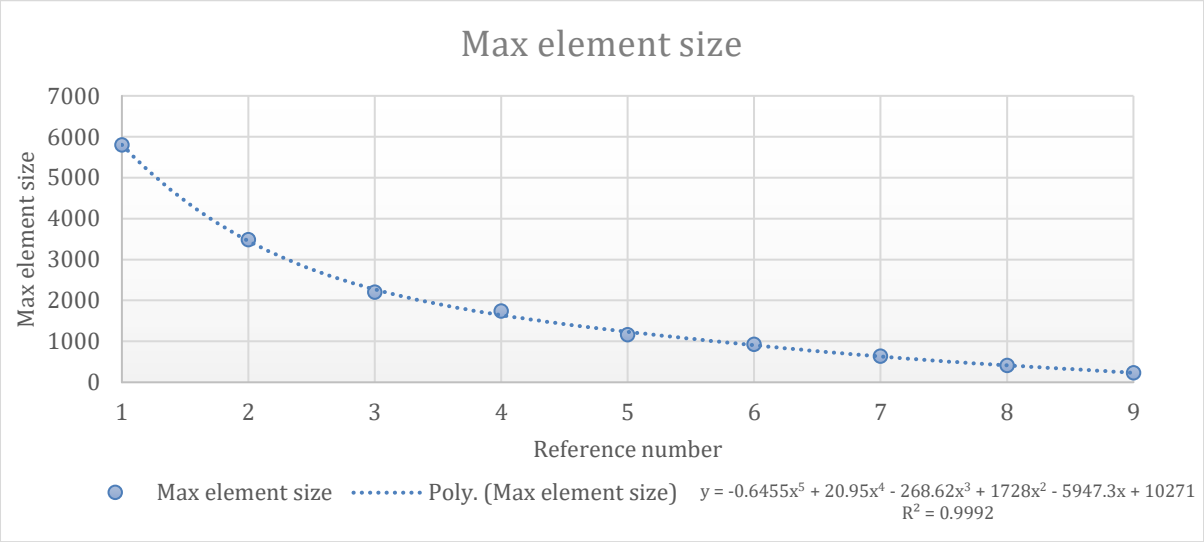

Figure 9.1.1 Pre-defined mesh size parameter *max element size* plotted against the reference number and its polynomial equation using trendline in Excel.

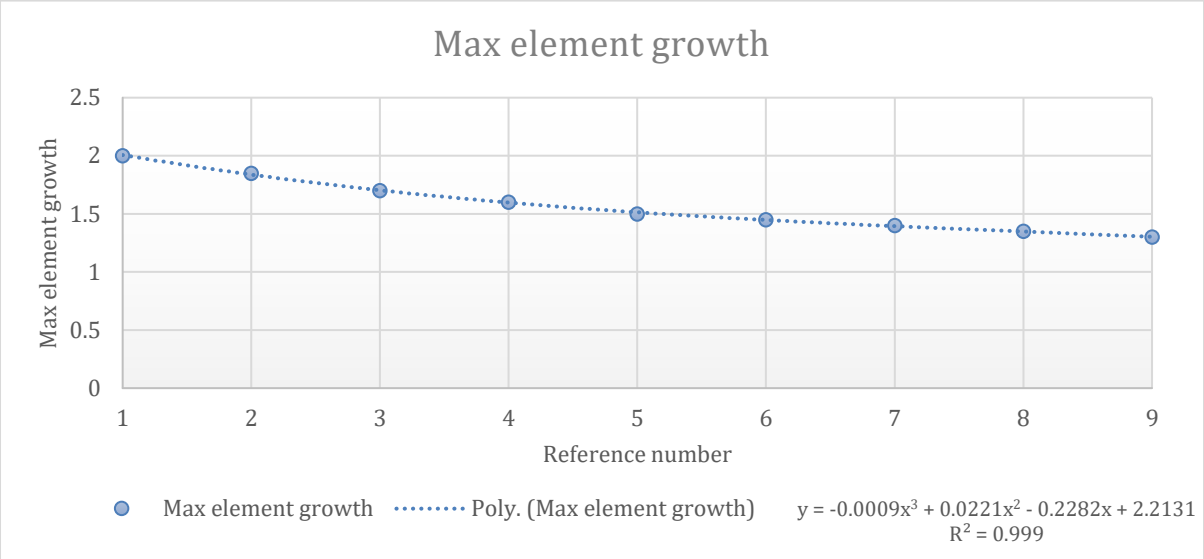

Figure 9.1.2 Pre-defined mesh size parameter *max element growth* plotted against the reference number and its polynomial equation using trendline in Excel.

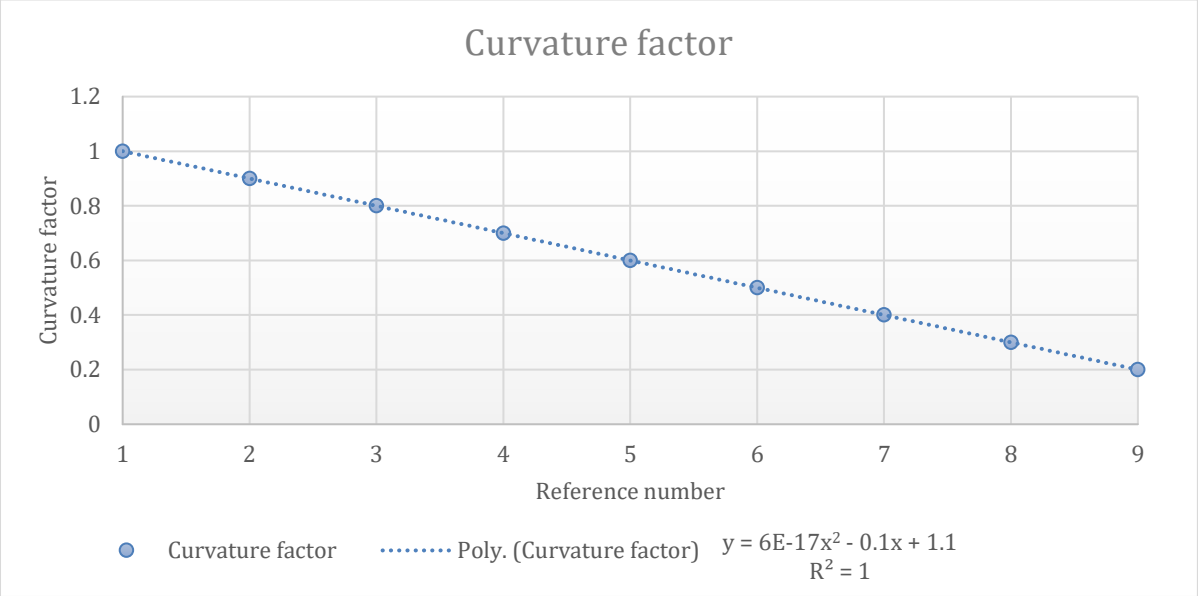

Figure 9.1.3 Pre-defined mesh size parameter *curvature factor* plotted against the reference number and its polynomial equation using trendline in Excel.

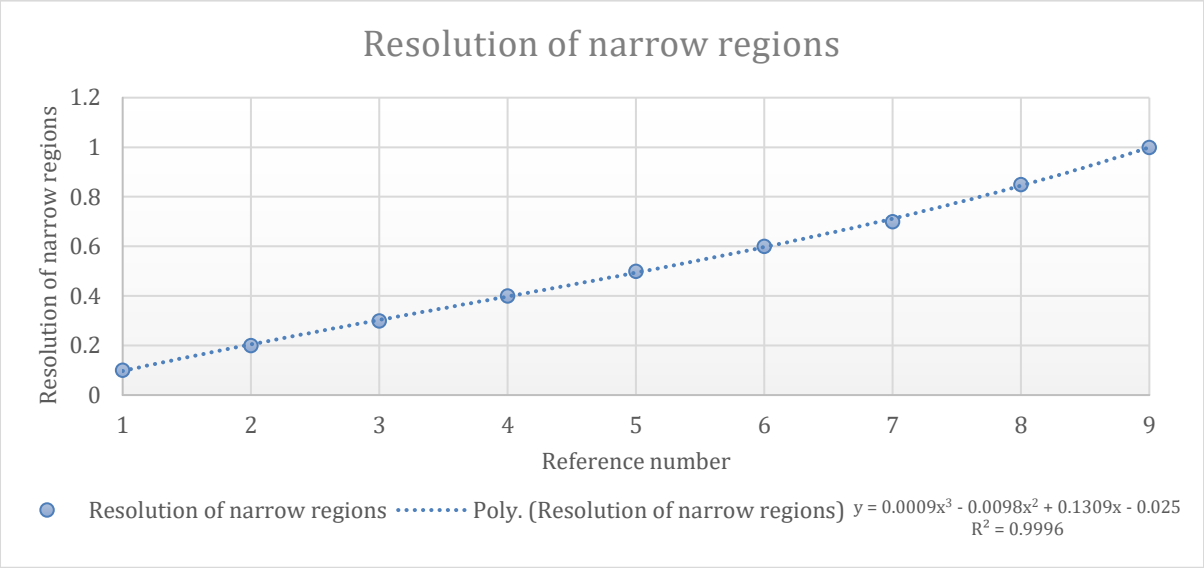

Figure 9.1.4 Pre-defined mesh size parameter *resolution of narrow regions* plotted against the reference number and its polynomial equation using trendline in Excel.

9.2 Appendix 2: Darcy Velocity range

Below is the Darcy velocity vertical component range at the top surface presented, the stream network which was provided by Mojarrad et al. (2021) is used in these illustrations.

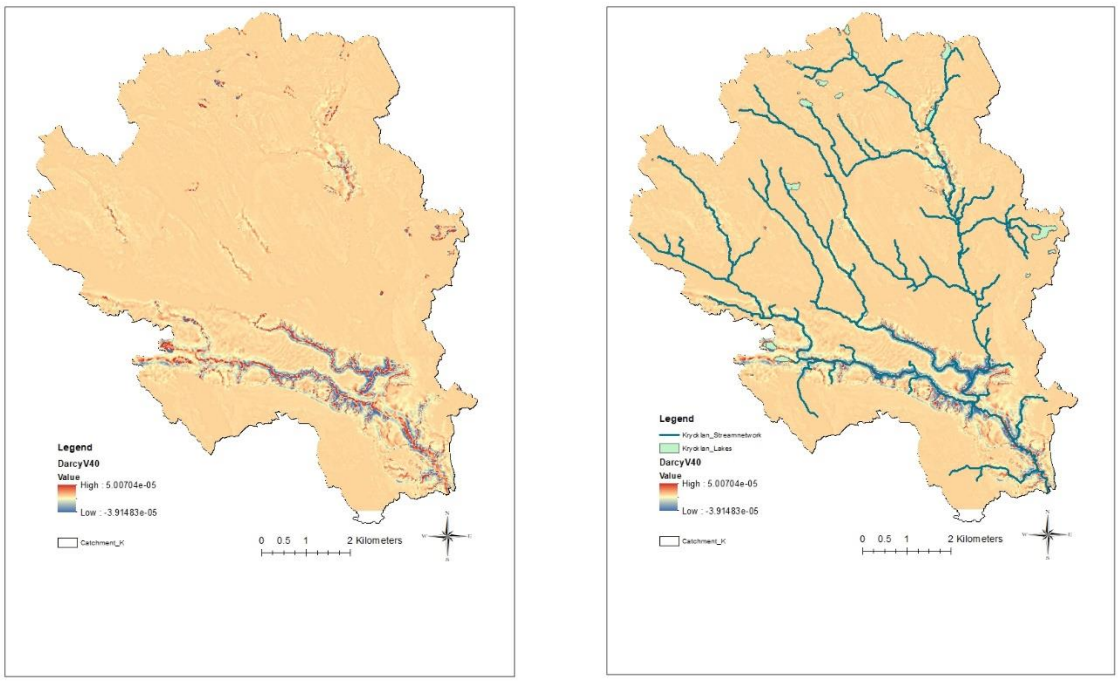

(a) **(b)**

Figure 9.2.1 Darcy velocity (m/s) range in Krycklan illustrated using ArcMAP, resolution 2x40 m. Without (a) and with (b) stream network and lakes in Krycklan catchment.

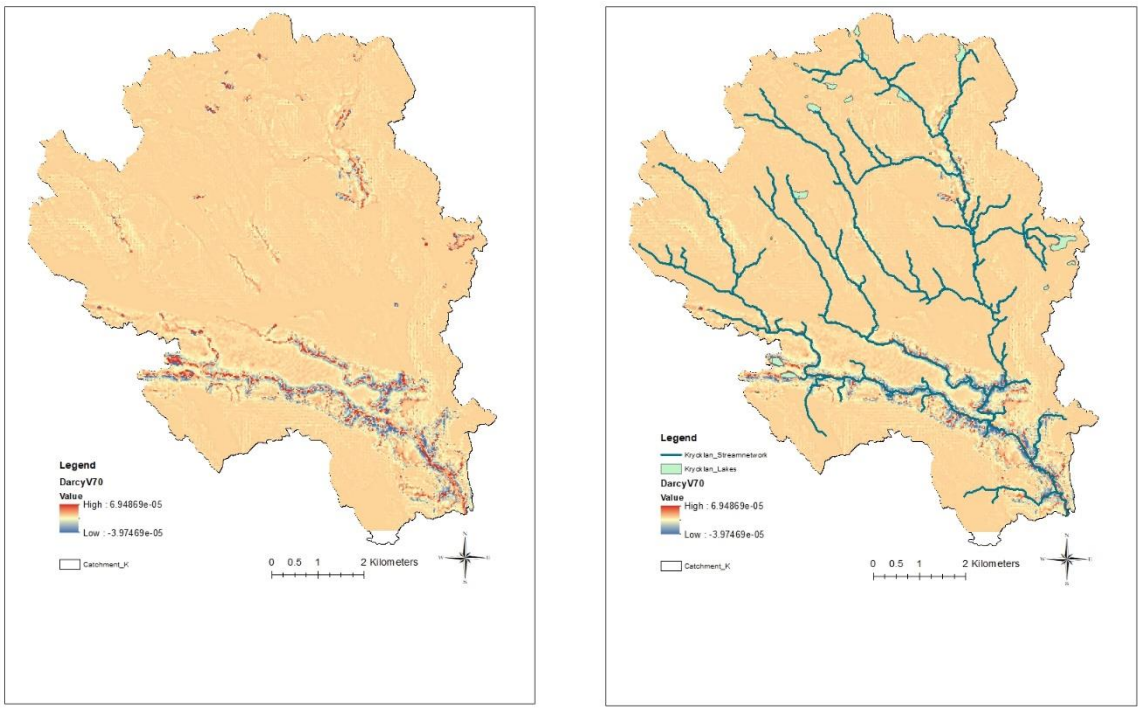

(a) **(b)**

Figure 9.2.2 Darcy velocity (m/s) range in Krycklan illustrated using ArcMAP, resolution 2x70 m. Without (a) and with (b) stream network and lakes in Krycklan catchment.

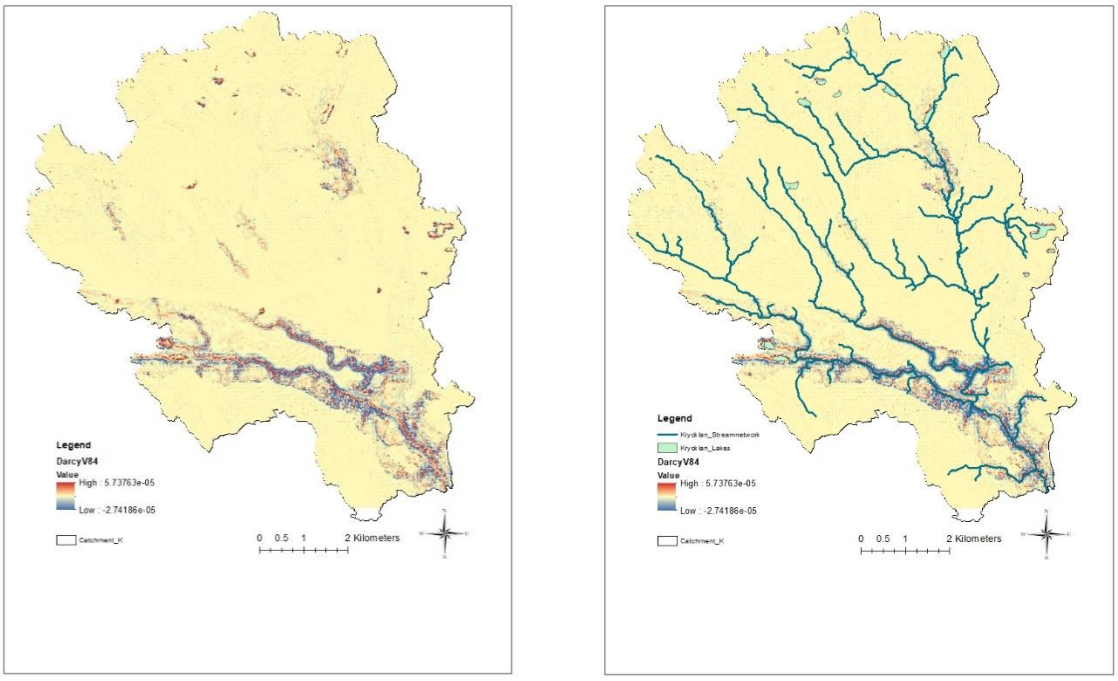

(a) **(b)**

Figure 9.2.3 Darcy velocity (m/s) range in Krycklan illustrated using ArcMAP, resolution 2x84 m. Without (a) and with (b) stream network and lakes in Krycklan catchment.

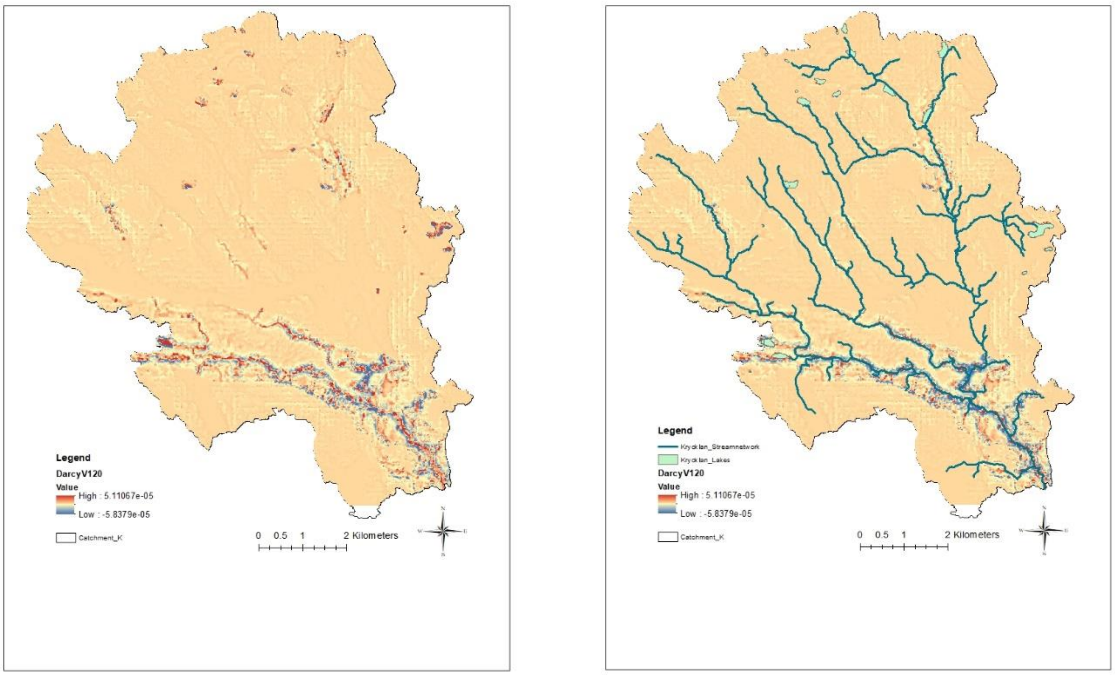

(a) **(b)**

Figure 9.2.4 Darcy velocity (m/s) range in Krycklan illustrated using ArcMAP, resolution 2x120 m. Without (a) and with (b) stream network and lakes in Krycklan catchment.

9.3 Appendix 2: Recharge and discharge areas

Below is the recharge and discharge areas presented, the stream network which was created with hydrological tools in ArcMAP is used in these illustrations.

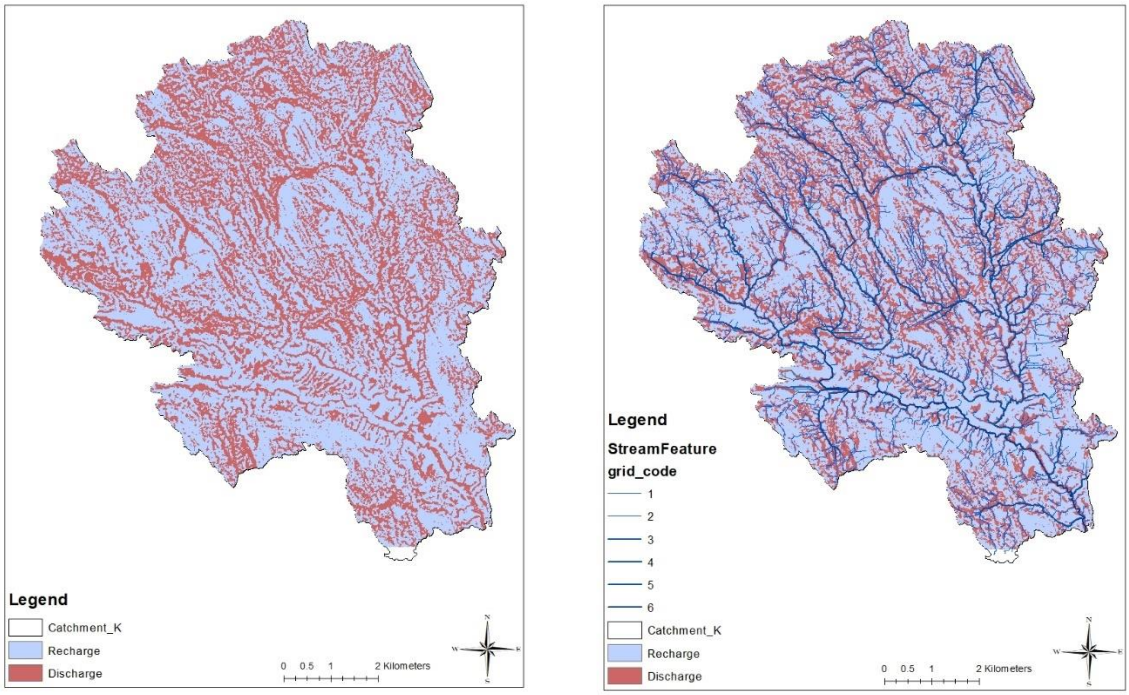

(a) **(b)**

Figure 9.3.1 Recharge and discharge areas in Krycklan illustrated using ArcMAP, resolution 2x40 m. Without (a) and with (b) stream network and lakes in Krycklan catchment. The thinner blue lines represents the lower ordered streams (1 & 2).

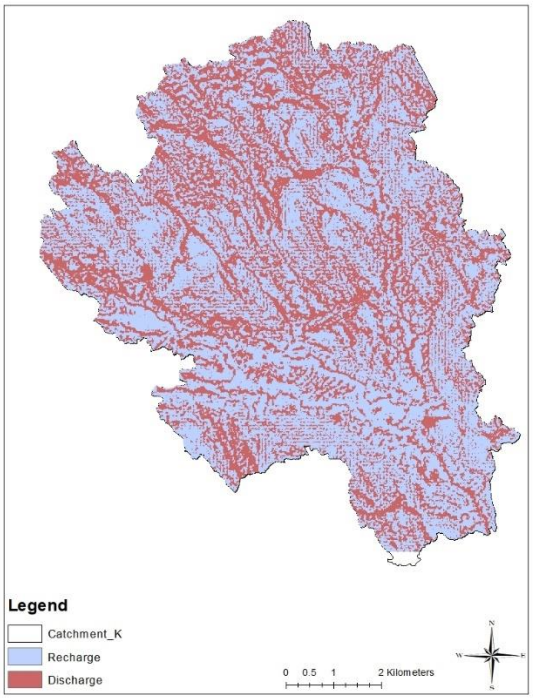

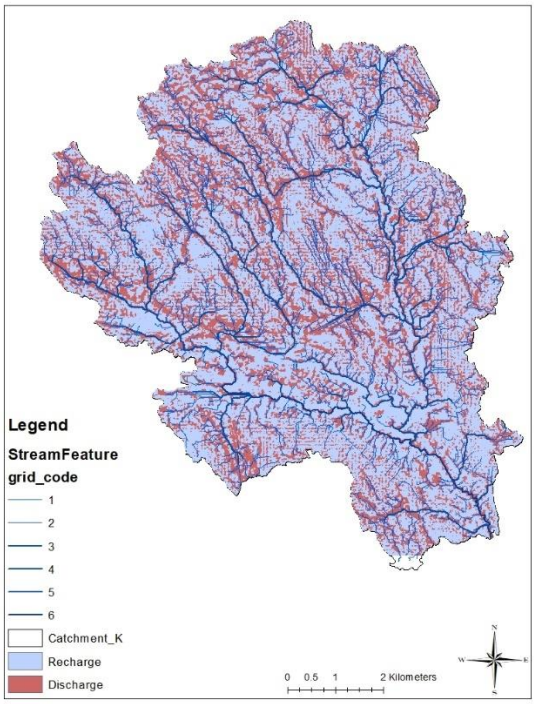

(a) **(b)**

Figure 9.3.2 Recharge and discharge areas in Krycklan illustrated using ArcMAP, resolution 2x70 m. Without (a) and with (b) stream network and lakes in Krycklan catchment. The thinner blue lines represents the lower ordered streams (1 & 2).

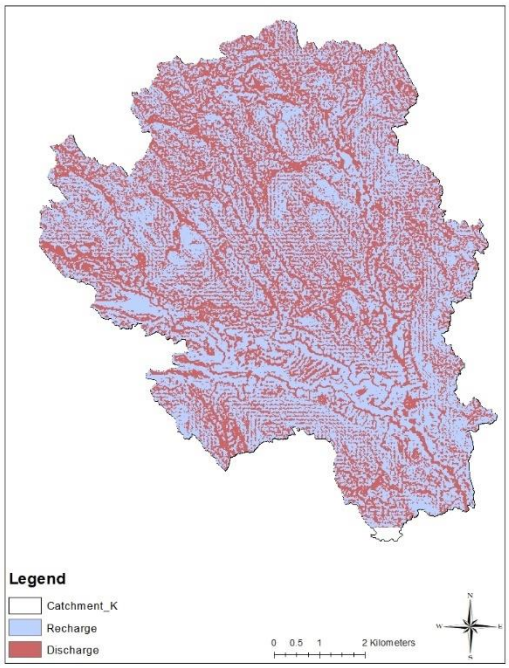

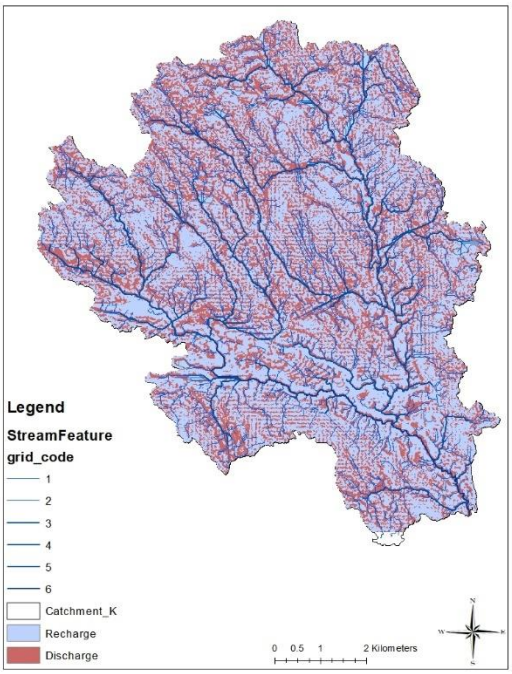

(a) **(b)**

Figure 9.3.3 Recharge and discharge areas in Krycklan illustrated using ArcMAP, resolution 2x84 m. Without (a) and with (b) stream network and lakes in Krycklan catchment. The thinner blue lines represents the lower ordered streams (1 & 2).

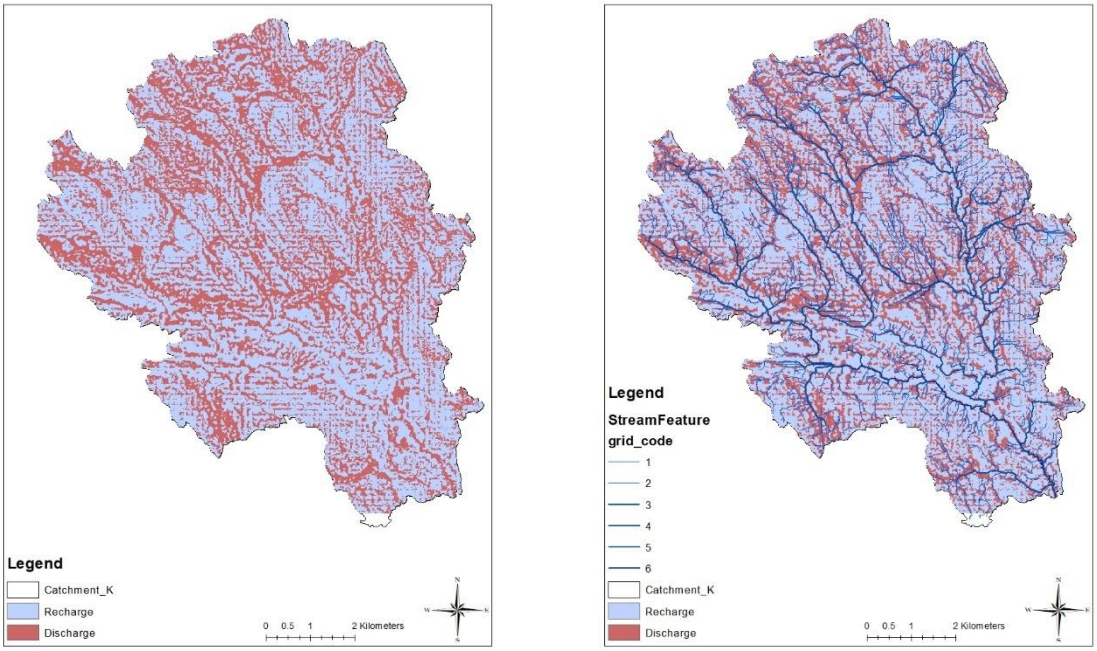

(a) **(b)**

Figure 9.3.3 Recharge and discharge areas in Krycklan illustrated using ArcMAP, resolution 2x120 m. Without (a) and with (b) stream network and lakes in Krycklan catchment. The thinner blue lines represents the lower ordered streams (1 & 2).

9.4 Appendix 3: Discharge distribution

Below is the discharge distribution of the discharge areas presented, the stream network which was created with hydrological tools in ArcMAP is used in these illustrations.

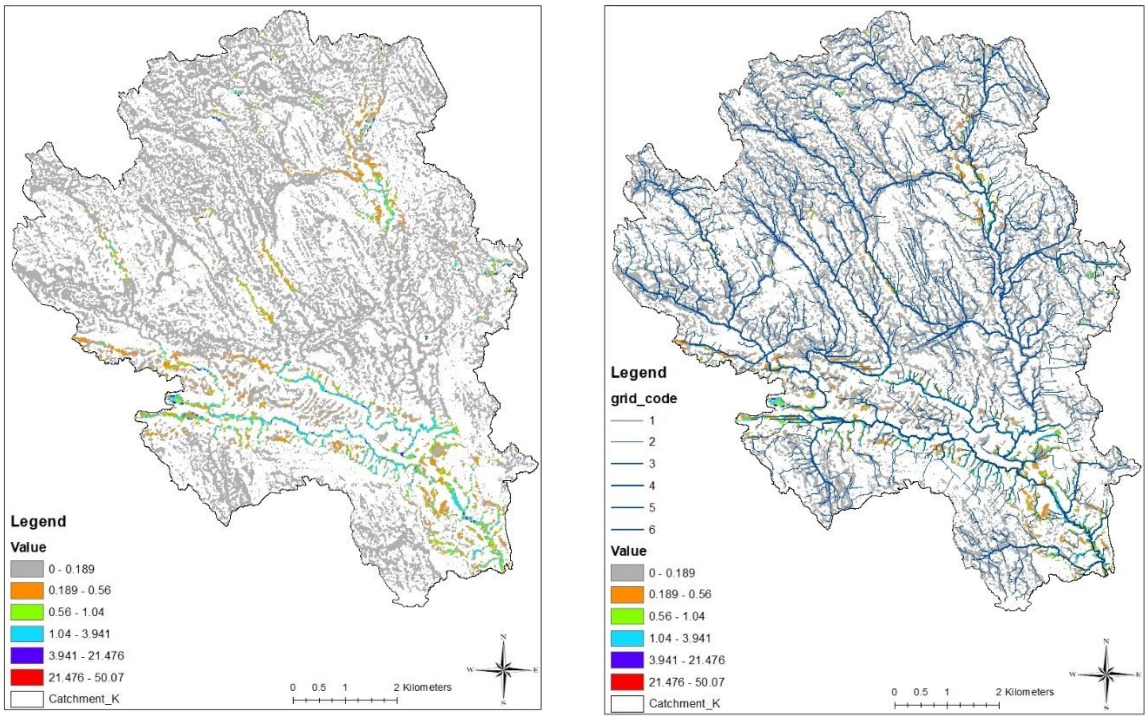

(a) **(b)**

Figure 9.4.1 Distribution of discharge velocities 10^{-6} (m/s) in Krycklan illustrated using ArcMAP, resolution 2x40 m. Without (a) and with (b) stream network and lakes in Krycklan catchment. The thinner blue lines represents the lower ordered streams (1 & 2).

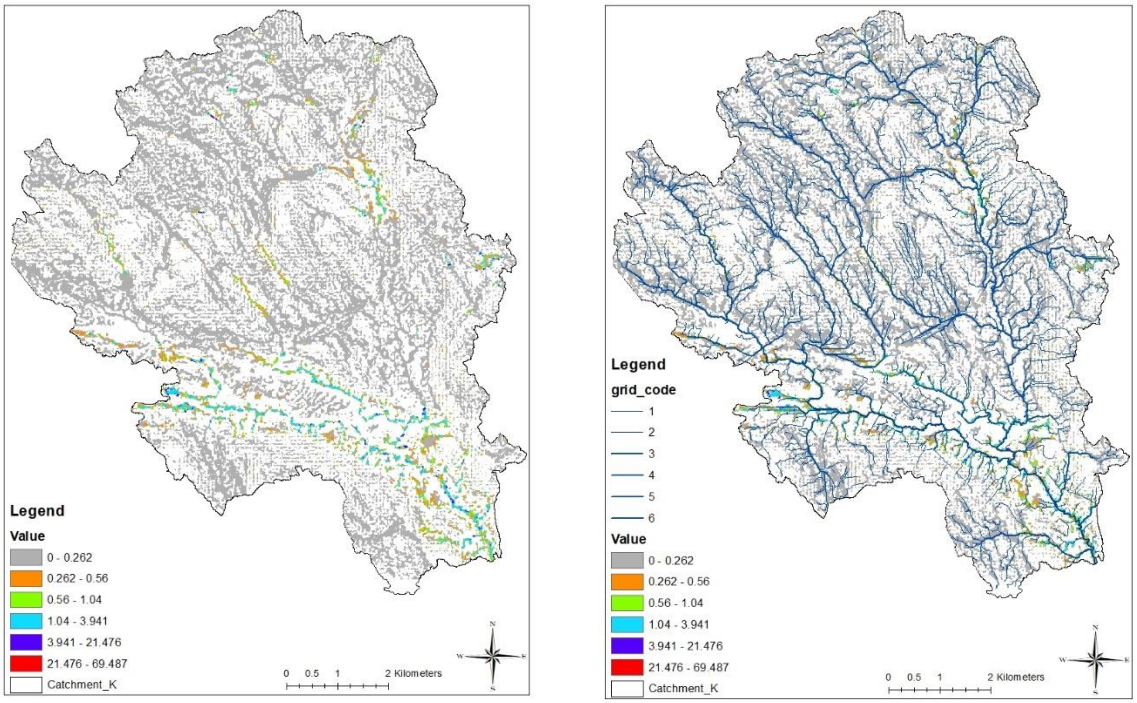

(a) **(b)**

Figure 9.4.2 Distribution of discharge velocities 10^{-6} (m/s) in Krycklan illustrated using ArcMAP, resolution 2x70 m. Without (a) and with (b) stream network and lakes in Krycklan catchment. The thinner blue lines represent the lower ordered streams (1 & 2).

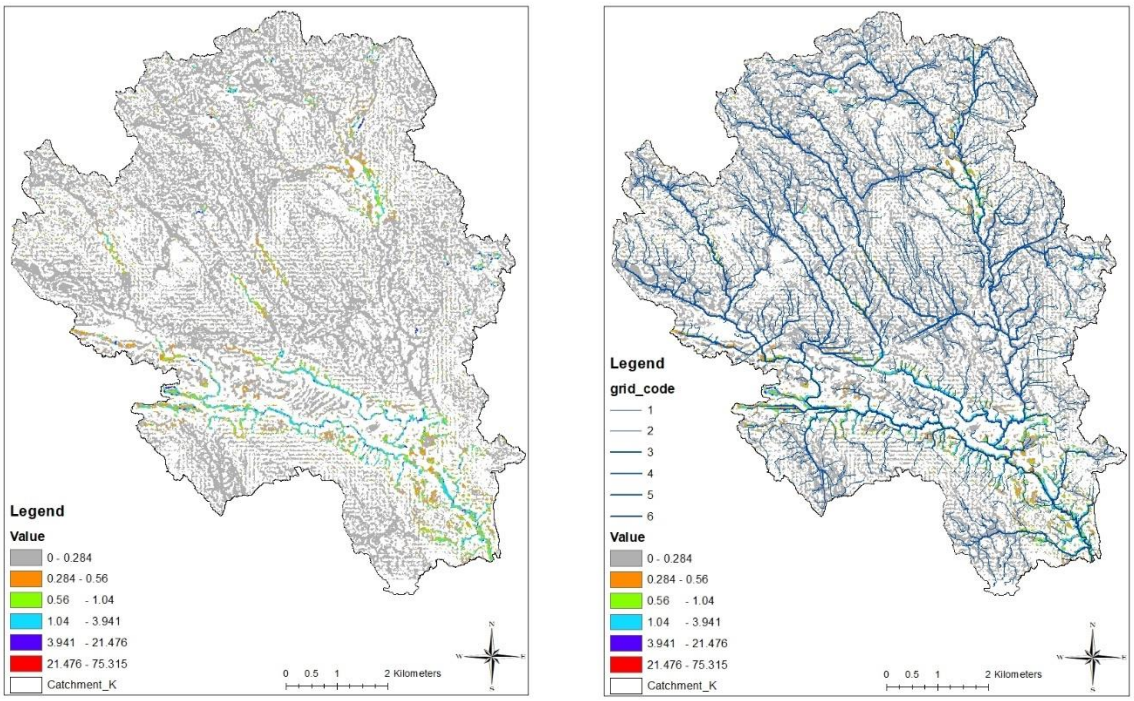

(a) **(b)**

Figure 9.4.3 Distribution of discharge velocities 10^{-6} (m/s) in Krycklan illustrated using ArcMAP, resolution 2x84 m. Without (a) and with (b) stream network and lakes in Krycklan catchment. The thinner blue lines represents the lower ordered streams (1 & 2).

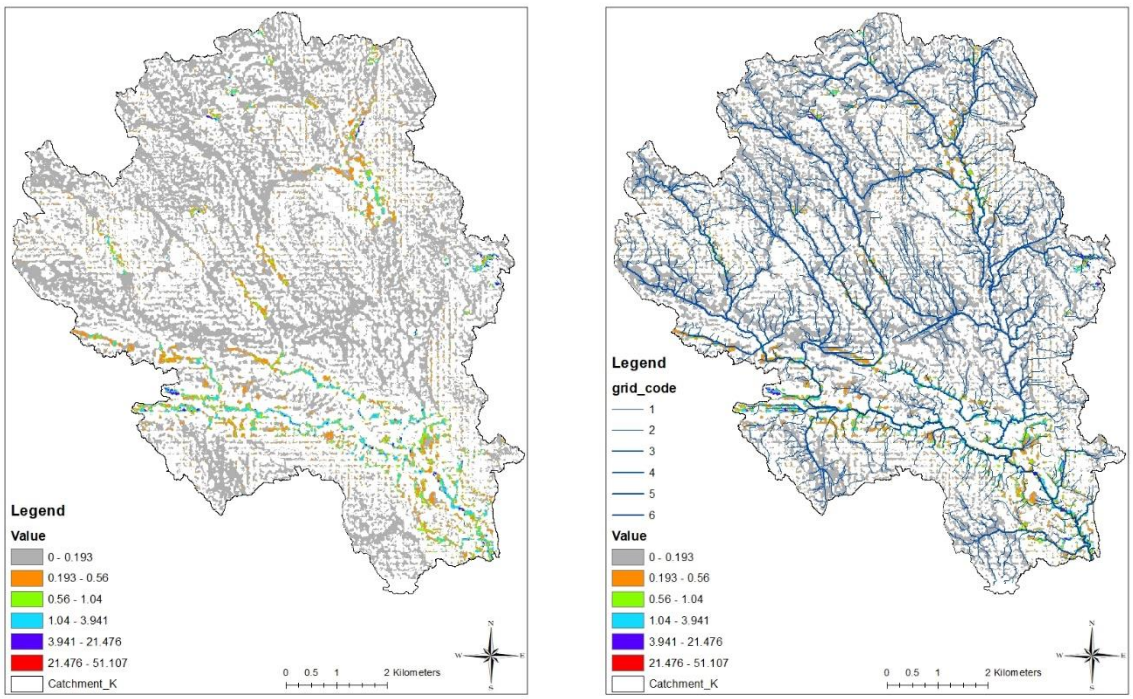

(a) **(b)**

Figure 9.4.4 Distribution of discharge velocities 10^{-6} (m/s) in Krycklan illustrated using ArcMAP, resolution 2x120 m. Without (a) and with (b) stream network and lakes in Krycklan catchment. The thinner blue lines represents the lower ordered streams (1 & 2).

9.5 Appendix 4: Discharge distribution of evapotranspiration balanced areas

Below is the discharge distribution of the evapotranspiration balanced areas presented, the stream network which was created with hydrological tools in ArcMAP is used in these illustrations.

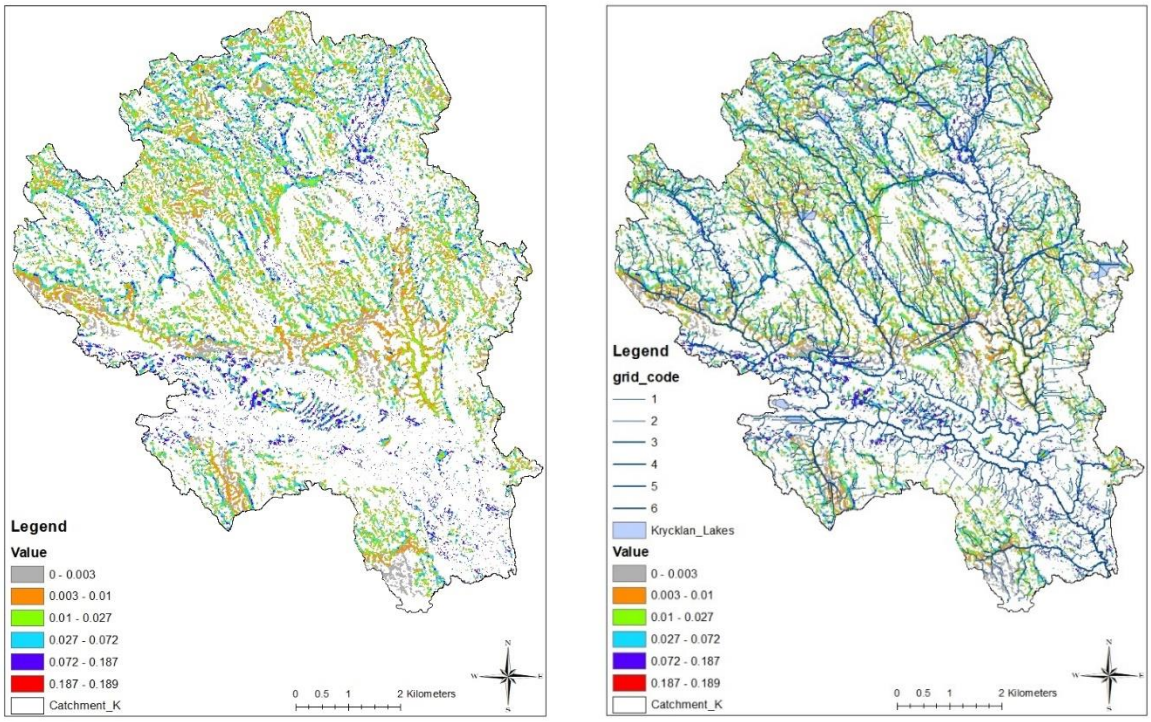

(a) **(b)**

Figure 9.5.1 Distribution of evapotranspiration discharge velocities 10^{-6} (m/s) in Krycklan illustrated using ArcMAP, resolution 2x40 m. Without (a) and with (b) stream network and lakes in Krycklan catchment. The thinner blue lines represents the lower ordered streams (1 & 2).

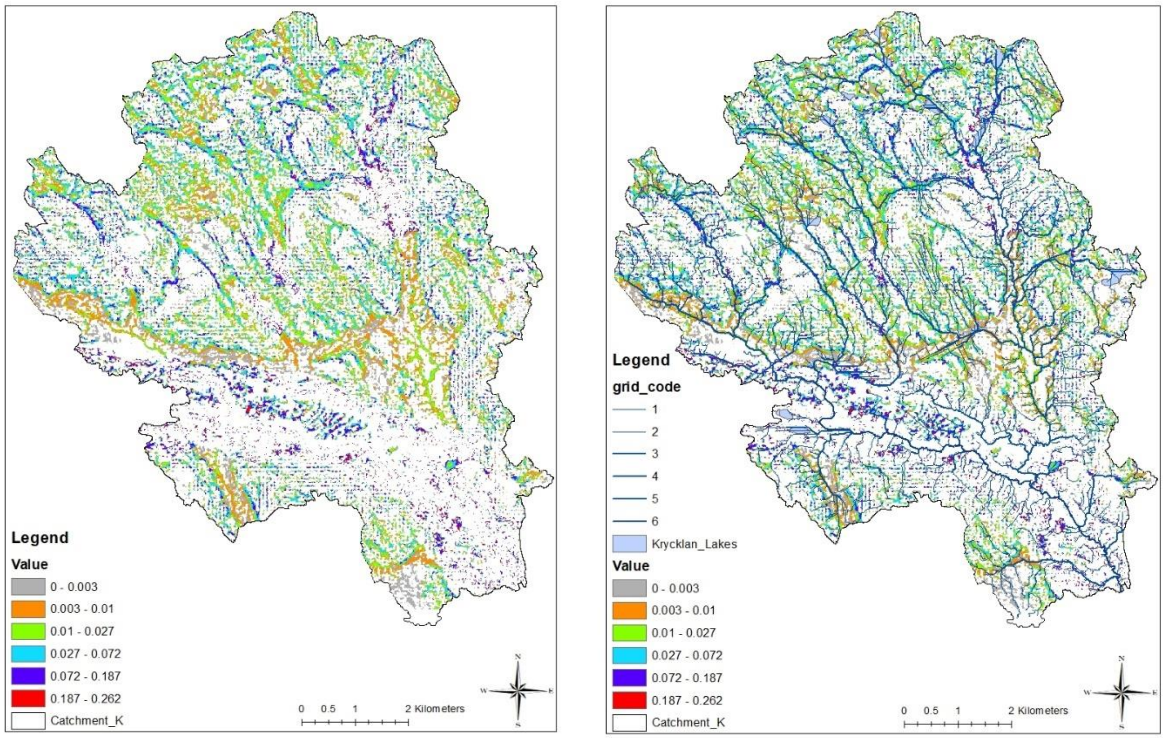

(a) **(b)**

Figure 9.5.2 Distribution of evapotranspiration discharge velocities 10^{-6} (m/s) in Krycklan illustrated using ArcMAP, resolution 2x70 m. Without (a) and with (b) stream network and lakes in Krycklan catchment. The thinner blue lines represents the lower ordered streams (1 & 2).

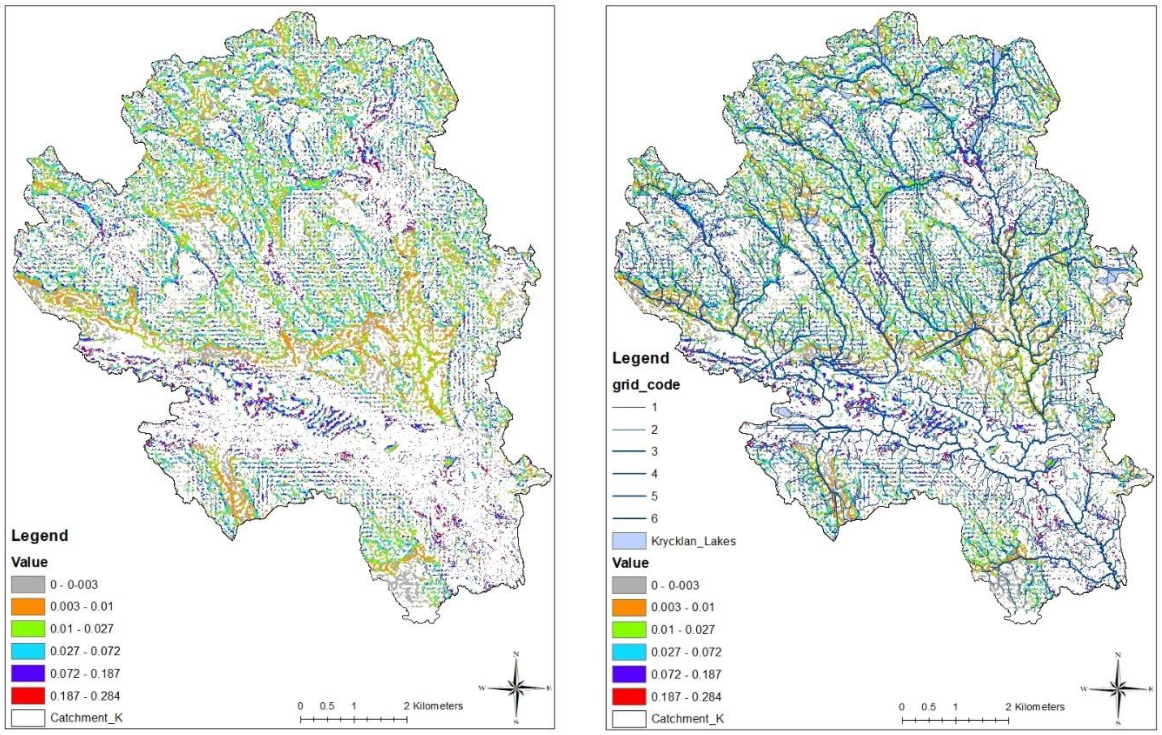

(a) **(b)**

Figure 9.5.3 Distribution of evapotranspiration discharge velocities 10^{-6} (m/s) in Krycklan illustrated using ArcMAP, resolution 2x84 m. Without (a) and with (b) stream network and lakes in Krycklan catchment. The thinner blue lines represent the lower ordered streams (1 & 2).

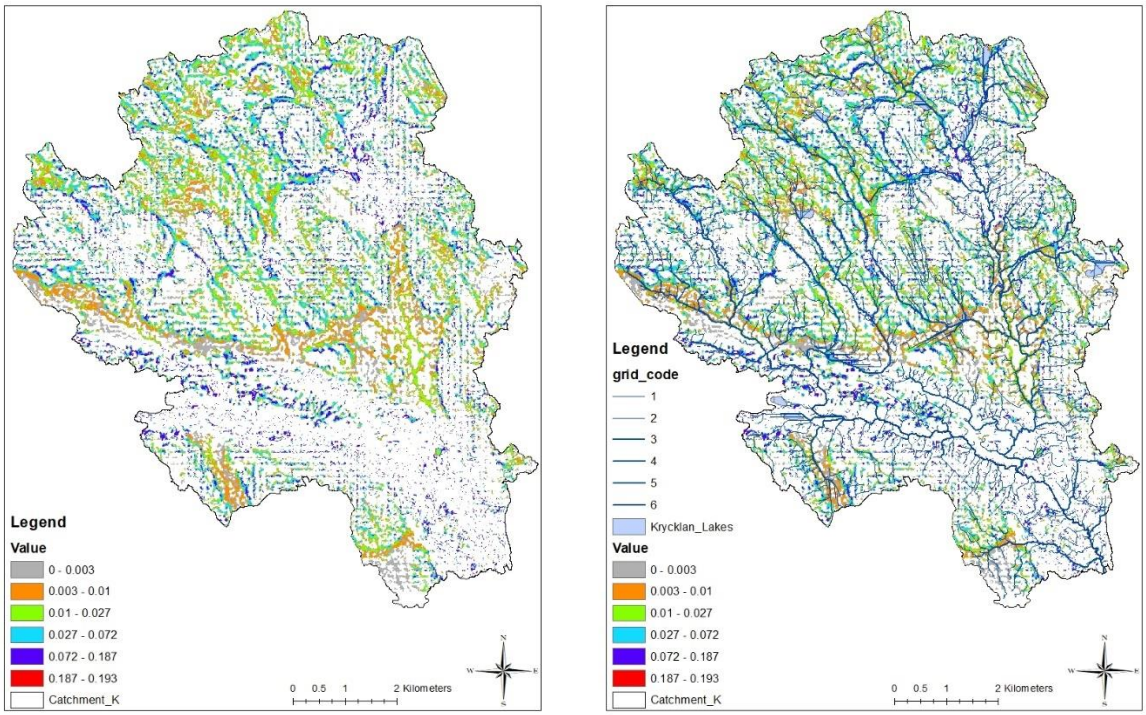

(a) **(b)**

Figure 9.5.4 Distribution of evapotranspiration discharge velocities 10^{-6} (m/s) in Krycklan illustrated using ArcMAP, resolution 2x120 m. Without (a) and with (b) stream network and lakes in Krycklan catchment. The thinner blue lines represents the lower ordered streams (1 & 2).

TRITA-ABE-MBT 22433